6-2021

Composite Analysis of Mendenhall Glacier Interannual Glacial Health Decline

Hailey Marie Cantrell
Western Michigan University, haileyc11@gmail.com

COMPOSITE ANALYSIS OF MENDENHALL GLACIER INTERANNUAL GLACIAL HEALTH DECLINE

by

Hailey Marie Cantrell

A thesis submitted to the Graduate College
in partial fulfillment of the requirements
for the degree of Master of Science
Department of Geography, Environment, and Tourism
Western Michigan University
June 2021

Thesis Committee:

Lei Meng, Ph.D., Chair
Lisa M. DeChano-Cook, Ph.D.
Yosef Mendelsohn, M.D.

COMPOSITE ANALYSIS OF MENDENHALL GLACIER INTERANNUAL GLACIAL HEALTH DECLINE

Hailey Marie Cantrell, M.S.

Western Michigan University, 2021

Glacial health in Alaska, USA is demonstrating an interannual declining trend. Repetitive years have suffered an imbalance between winter seasonal ice accumulation and summer seasonal ice loss. Increased ice loss has commonly been attributed to warmer Arctic summer temperatures, which contribute to greater calving events and amplified ablation. Study of the unique climatic influences by different variables is ongoing and at the forefront of climate-glacier interaction research.

This study is designed to quantitatively evaluate correlations between changes in Alaskan climatic patterns and an interannual trend of declining glacial health for Mendenhall Glacier by combining analysis of Landsat satellite imagery, teleconnection data for the Arctic Oscillation, the Southern Oscillation, and the Pacific Decadal Oscillation, sea surface temperature anomalies, and Alaskan climatological data. Neither the expected significant relationship between glacier area loss and the Arctic Oscillation nor between glacier area loss and summer seasonal temperatures are reflected in the results of this analysis. However, the results of this study do suggest a significant correlation between Gulf of Alaska sea surface temperatures and glacier area loss along the southeastern coastline of Alaska, represented here by a specific look at Mendenhall Glacier.

ACKNOWLEDGMENTS

Throughout this process I have received encouragement and support from many individuals, but I would like to take the time to name a few who have been instrumental in my success. First, I would like to extend my gratitude to Dr. Kelsey Ellis at the University of Tennessee Knoxville and Zachary Merrill for their support and faith during my senior year of undergraduate studies. Without their encouragement and guidance, I would not have embarked on this journey. I would also like to thank Daniel Burow, who encouraged me along the way and provided the opportunity for me to be a co-author with him, giving me my first publication.

I would like to sincerely thank the faculty and staff, including those who have since retired, in the Department of Geography, Environment, and Tourism at Western Michigan University, namely Dr. Benjamin Ofori-Amoah, Dr. Lei Meng, and Dr. Lisa DeChano-Cook. I would like to thank Dr. Ofori-Amoah for seeing the potential in me when I was just an ambitious Geography minor and for offering me this opportunity. I have deep gratitude for Dr. Meng and Dr. DeChano-Cook, from whom I have learned so much about science and about my passions in academia. I would also like to thank Dr. Yosef Mendelsohn of DePaul University, a dear friend and diving buddy who stepped up to serve on my committee from afar during these unprecedented times.

Finally, I would like to deeply thank those closest to my heart. I would like to thank Robert Lyczynski. Without his love, support, and mindfulness to keep me focused and on track, I very well may have given up when the going got tough. I would like to thank my grandfather, Dr. Max Hailey, and Sarah. Their love and phone calls always brightened my days and gave me

encouragement. My grandfather's experiences in academia and wisdom were guidance for me through much of this process. Lastly, I want to thank my immediate family for countless cards and calls, for patiently listening to me ramble, rant, cry, and laugh, and for unconditionally loving and supporting me in every way to succeed. I would not be who I am without them, and I have missed them while "way up here in the cold north," as my father would say.

My growth as a person and scholar throughout my studies is thanks to these individuals, and my deepest gratitude is extended to them.

Hailey Marie Cantrell

TABLE OF CONTENTS

Table of Contents – Continued

Table of Contents – Continued

CHAPTER

LIST OF TABLES

LIST OF FIGURES

List of Figures – Continued

CHAPTER I

INTRODUCTION

Glacial health in Alaska is demonstrating a declining trend. Glacial health is defined for the purpose of this study as the interannual condition of net volumetric ice balance. Positive glacial health necessitates temporal stability in glacier growth and retreat rates. Negative glacial health is a disproportionate ratio of glacier retreat to glacier growth over a series of years, historically measured at the end of summer melt periods. Historical photographic evidence of Mendenhall Glacier, Alaska, undoubtedly exhibits the consistent pattern in interannual glacial retreat when compared to contemporary imagery (Figures 1 and 2). Studying climatic forcings driving this pattern of glacial movement is relevant and crucial for better understanding of future glacial behavior attributed to anthropogenically-driven climate change.

Of the commonly discussed risk factors of climate change, such as tropical cyclone intensification, increased drought duration, and the weakening of the thermohaline circulation, which leads to more extreme temperatures, anticipated sea-level rise is perceived by many as the most dangerous and relevant (VanLooy and Vandeberg 2019; Nicholls and Cazenave 2010; Xu *et al.* 2009). The two main contributing factors to sea-level rise are thermal expansion of ocean waters and increased water mass input from land ice melt. Two-thirds of the observed sea-level rise since the 1990s is credited to ice mass loss from ice sheets and glaciers (Dunse *et al.* 2015). Nicholls and Cazenave (2010) stated that polar ice sheet mass has an accelerated decline from that which was released in the Fourth Assessment Report of the Intergovernmental Panel on Climate Change, raising predicted sea-level rise to one meter or more by 2100. This is likely attributed to the potential dynamic response of ice velocity to climate change (Dunse *et al.*

Figure 1. 1958 Mendenhall Glacier terminus. Photograph of the Mendenhall Glacier terminus, as seen from "Mal's Photo Point," taken in 1958 by Marrion T. Millet. The region shaded in red identifies the current range of seasonal glacial movement. Source: After GlacierChange.org 2011

Figure 2. 2019 Mendenhall Glacier terminus. Photograph of the Mendenhall Glacier terminus, as seen from "Mal's Photo Point," taken in July 2019. Source: Primary source photograph by author

2015). Not only does anthropogenically-induced glacial melting contribute to rising sea-levels, it also affects flood plains, freshwater availability, agricultural irrigation, and downstream soil fertility attributed to glacial outwash minerals (VanLooy and Vandeberg 2019; Xu *et al.* 2009).

Another implication of climate-driven glacial change is the increased risk of glacial surges. A surge event is defined as "a sudden speedup of glacier flow coinciding with a large advance of the ice front" (Zheng et al. 2019, pg. 13892). The rapid forward ice flow is 10 to 100 times the speed of quiescent (normal) flow of the glacier (Burgess *et al.* 2012). Glacial surges are hazards that occur due to favorable conditions resulting from long periods of precipitation and temperature increase, and they pose threats to societies or agricultural land in their path. They are triggered by hydrological instability and vary in duration, lasting months to upwards of several years, often initiating and terminating very suddenly (Yao *et al.* 2019; Burgess *et al.* 2012). Climatic and geometric factors, such as temperature regimes, underlying hydrological conditions, and slope, control glacial surge-potential spatial distribution. Sevestre and Benn (2015) used an updated global geodatabase of 2317 surge-type glaciers to identify correlations between their spatial distribution, site-specific climatic factors, and glacier geometry variables. Ideal thresholds of mean annual temperature of -10 degrees Celsius to 0 degrees Celsius and mean annual precipitation of 30–2250 mm a^{-1} yield the highest density clusters of surge-type glaciers (Sevestre and Benn 2015). Warming polar summer temperatures contribute to an increase in glaciers that will fall within the ideal threshold for glacial surge.

Awareness of the implications of declining glacial health is key for ongoing academic interest in the field of climate-glacier interactions. Coastal populations run the inherent risk of being inundated by sea-level rise. In many areas, flooding and storm surges have become commonplace, and, as polar ice sheets melt, sea-level will continue to rise and freshwater reservoirs will cease to be replenished. Identifying influences of specific climatic variables on increased glacial melt and studying the current and changing trends of these variables will aid in

planning and mitigation efforts to combat the dangerous implications of glacial health decline as scholars will be able to better predict glacier response.

The need for continued research is evident. Mendenhall Glacier provides an ideal backdrop for studying the relationship between glacial geomorphology, climatic influences, and glacial health trends and is representative of much of the glacial landscape of Alaska's southeastern coastline. The purpose of this proposed study is to quantitatively determine a correlation between changes in Alaskan climatic patterns and an interannual trend of declining glacial health. Specific research questions to be addressed are:

1. Is there a significant correlation between summer seasonal temperature maximum means and glacier area loss?
2. Is there a significant correlation between summer seasonal temperature maximum means and the rate of area loss?
3. Is there a significant correlation between the Arctic Oscillation, the Southern Oscillation, and/or the Pacific Decadal Oscillation and glacier area loss?
4. Is there a significant correlation between the Arctic Oscillation, the Southern Oscillation, and/or the Pacific Decadal Oscillation and the rate of area loss?
5. Is there a significant correlation between Gulf of Alaska sea surface temperature anomalies and glacier area loss?
6. Is there a significant correlation between Gulf of Alaska sea surface temperature anomalies and the rate of area loss?

This thesis is organized into the following chapters: 1) a comprehensive background on the geomorphological processes of Alaskan glacial systems; 2) a review of precedented climate-glacier interaction research; 3) data that were collected and methods of analysis for this study; 4)

results of analysis and discussion; and 5) a conclusion of this research's implications and areas open for further research.

CHAPTER II

BACKGROUND

This chapter provides contextual background information on coastal Alaskan geomorphology with a focus on glacial systems. It further identifies the root causes of glacial growth through accumulation and glacial retreat through calving and ablation.

Geomorphology of coastal Alaskan glacial systems

The southern Alaskan coastline is a narrow plain bordered to the north by the Chugach and St. Elias Mountains and features two distinct geomorphological forms: 1) glacial outwash plains and 2) river deltaic systems (Hayes *et al.* 1976). The latter is encompassed by the Copper River delta, found to the west of Alaskan glacial systems and not a factor of regional glacial movement (Figure 3). Alaskan coastal glacial systems are unique to the Arctic polar region and are representative of coastal glaciers in Canada, Greenland, and Eurasia.

The southern shoreline of Alaska is classified as geomorphologically unstable, meaning that the shoreline is constantly changing. Glacial retreat has given rise to unpredictable erosion, outwash sediment deposition, and isostatic rebound, which is an uplifting of the land surface (Larsen *et al.* 2004; Hayes *et al.* 1976). As previously noted, the primary geomorphologic land-type dominating the southeastern coast of Alaska is a glacial outwash plain, which is a system of outwash flows with downstream beach-ridge plains. The glacial outwash plain can be subdivided into five categories: 1) regional retreating coasts; 2) prograding sandy spits; 3) abandoned glacial coasts; 4) actively eroding glacial margins and; 5) glacial outwash coasts (Hayes *et al.* 1976).

Figure 3. Geography of the southeastern Alaskan coast. This map provides the regional geography of the southeastern Alaskan glacial landscape relative to the Copper River Delta and the Yukon Territory of Canada.

Regional retreating coasts are the result of a glacial retreat that leaves in its wake a rapidly eroding, unstable coastline. Prograding sandy spits are the result of shoreline erosion at the mouth of glacial bays. Abandoned glacial coasts are the most stable regions and experience low rates of erosion, minimal storm influence, and are often highly vegetated. Actively eroding glacial margins protrude into the Gulf of Alaska and are the most unstable regions as they exist on the southernmost glacial extents. Glacial outwash coasts are prograding shoreline regions that are rapidly variable and influenced in large-part by sediment movement (Hayes *et al.* 1976). Each of these categories of glacial outwash plain have unique characteristics, but generalizations can be made on the influence of climate on the southeastern Alaskan glacial landscape and the response of ice flow and glacial melt.

Climate variability and ice flow

Understanding the relationship between climate change, ice flow, and melt supply is an integral step in predicting potential glacial outwash locations. Ice velocity is the rate at which ice mass is moved to a glacial front and is a determining factor in the relationship between ice flow and melt supply. Glacial ice flow dynamics are often calculated under the assumptions of polar ice sheet mass-balance equilibrium and ice flow perpendicular to surface contours, neglecting the influential gravitational factor (Rignot *et al.* 2011). The primary ice flow method for Alaskan glaciers is basal-slip motion. This method of motion is based on tributary flow through and under the glacier, rather than deformation-dominated ice sheet flow, and demonstrates the origin of ice sheet movement at topographic divides, such as crevasses where water can be channeled through the glacier.

Basal-slip motion is caused by channeling thicker ice through subglacial valleys. This generates substantially more friction, therefore more heat and more ice melt underneath the glacier. Increased ice melt provides a lubricant for glacial movement and dampens sediments, enabling erosion and ice flow over glacial till (Rignot *et al.* 2011). This basal morphology provides a deformable bed, and, when paired with disruption to the hydraulic system of the glacier, prime geomorphic conditions for a glacial surge (Harrison and Post 2003).

In North American glacial systems, surge-type glaciers are predominately found in Alaska and the Yukon Territory of Canada (Lingle *et al.* 1993). All surge-type glaciers in Alaska have been observed to occur over glacial till beds where this easily eroded material facilitates swift ice flow (Harrison and Post 2003). Basal bedrock erosion rate during a glacial surge is directly proportional to the high ice velocity, meaning there is significantly more sediment movement and geomorphic change under and along the glacier than during quiescent

flow (Humphrey and Raymond 1994). During quiescent flow, which typically lasts for decades, ice velocity is slower than balance velocities, causing a thickening of ice in the accumulation zone and thinning in the ablation zone. This steepening of glacier geometry contributes to the initiation of a surge event, which flattens the geometry with the accelerated ice flow and resets the glacier for another extended quiescent phase (Burgess *et al.* 2012).

Climate variability strongly influences ice velocity and the ice flow dynamics of Alaskan glaciers. Anthropogenic climate change is increasing the range of Arctic summer temperatures, leading to changing glacial melt patterns. The subsequent increase in the variability of water input through glacial ice channels leads to an accelerated forward ice flow (Schoof 2010). Near-surface, englacial, and subglacial water flow are interconnected, and surface melt water flow has been recently observed to take an active role in ice flow acceleration (Dunse *et al.* 2015; Fountain and Walder 1998). For surge-type Alaskan glaciers, climate variability influences surge recurrence intervals by directly affecting surge initiation, termination, and magnitude, particularly through changes to temperature-based surface melt (Dunse *et al.* 2015; Harrison and Post 2003). A hydro-thermodynamic feedback system is triggered by surface melt as it reaches the glacier bed. This provides heat through cryo-hydrological warming and a change from cold to temperate basal conditions, allowing for basal slip-motion (Dunse *et al.* 2015).

Climate warming is increasing ice velocity and accelerating forward ice flow. Additionally, warming Arctic temperatures contribute to potentially more glacial surges. More surge events will change glacial bedrock geometry and the geomorphology of the southeastern Alaskan coastal region (Humphrey and Raymond 1994).

Root causes of glacial movement

Mass accumulation

Accumulation is the dynamic process by which glaciers gain ice mass. Direct accumulation involves the process of transforming snowfall on the surface of the glacier to firn and ultimately to ice. Firn is partially compacted snow that is undergoing melt and recrystallization under the pressure of newer snow. This process breaks the individual snowflakes and results in glacial ice over the period of approximately one year (NSIDC 2020a).

There is a distinct, coupled relationship between regional meteorological conditions and annual snow accumulation, much of which is based upon a glacier's physical location and geographic surroundings. Regions with extensive shade coverage and large ice expanses at high elevations promote healthy growth (Brocklehurst 2013). The majority of accumulation is attributed to direct snowfall on the glacier surface, but other factors can play a role. For example, wind or avalanches may either provide additional material to the glacier or remove snow and firn (Brocklehurst 2013; Sharp 1951). Other contributions to accumulation may come in the form of hail, though only a minor influence, or arien deposits, such as hoarfrost or rime, in maritime regions with high air moisture content (Sharp 1951).

Internal accumulation, though considered by some as a continuum of direct accumulation, is another method by which glaciers grow. Internal accumulation is differentiated by being a process where mass is redistributed within the glacial structure from its origin on the surface before being converted to glacial ice and occurs in glaciers with porous firn at sub-freezing temperatures that is penetrated by water. These glaciers are often found in cold continental or temperate maritime climates, where meltwater runoff is delayed and the conversion to glacial ice can be accelerated. Rain can serve as a source of accumulation but

must fall on snow or firn with sub-freezing temperatures causing the rain to freeze as it moves downward into the glacial structure. Meltwater can likewise serve as internal accumulation by refreezing within the glacier (Trabant and Mayo 1985; Sharp 1951). The process of internal accumulation is common for Alaskan glaciers, with particular influence in the northern extent of the state and decreasing in percent of total accumulation as one moves south (Trabant and Mayo 1985).

Mass loss

The two primary processes by which glaciers lose mass are through calving events and ablation. Glacier calving is the detachment of portions of ice, typically from the glacial terminus. The mechanics of glacier calving events are not well understood, and there are no conclusions or models that are universally accepted. What is known for certain is that crevasse depth and location, basal morphology, and removal of backstress on the terminus all have a role to play, and calving rates can substantially increase in response to ice velocity increases and/or retreat of the glacial terminus (Murray *et al.* 2015; Benn *et al.* 2007).

In more recent years, the Alaskan glacial landscape has seen the rise of large-scale glacier detachments. These detachments are primarily affecting valley glaciers with soft till beds, common characteristics along the glacial landscape of the southeastern coastal region. The large-scale detachments are comparable to massive calving events where substantial portions of the active glacier terminus break from the glacier bed and result in hazardous mass flows of ice, rock, and sediment (Jacquemart *et al.* 2020).

These events are a new concern to the glaciology community because detachments of this scale are unprecedented. The question that has begun to circulate is "…whether anthropogenic climate change is not only accelerating glacier retreat, but also introducing a previously

unobserved yet catastrophic mechanism of glacier destruction" (Jacquemart *et al.* 2020, pg. 703). The majority of Alaska's glaciers may be susceptible to these events as they are commonly valley glaciers. Presently for these glaciers, calving is a dominate force driving mass loss for ice sheets and tidewater terminating glaciers in particular (Murray *et al.* 2015). Though lake-terminating glaciers can and do undergo calving events, their primary form of mass loss is ablation.

Ablation is mass loss through the melting and subsequent evaporation or runoff of glacial ice, firn, and snow. Net ablation is the amount of mass actually removed from the glacier, but it is extremely difficult to measure, as meltwater may refreeze through the internal accumulation process. Therefore, gross ablation, the total amount of melting and evaporation, is often the focus of research. Additionally, gross accumulation is more relevant to the study of the thermal regimen, the formation of ice layers, and the movement of meltwater through firn (Sharp 1951).

Internal ablation can occur in crevasses, ice caves, and tunnels, but the majority of mass loss is via surface ablation, which can be influenced strongly by meteorological conditions or physical conditions such as large, shadowed regions of the glacial surface (Brocklehurst 2013; Sharp 1951). Unlike calving events, which do not affect all glaciers on a global scale, surface ablation is the primary method of mass loss for all categories of glaciers. Ablation rates and percent mass loss by ablation varies per glacier. As previously noted, within the Alaskan glacial landscape there are various categories of glaciers, with lake-terminating glaciers losing the largest percentage of mass by ablation. As Arctic temperatures warm and the insolation budget changes in favor of increased glacial melt, surface ablation will serve as a predictable mechanism for mass loss compared to the uncertainties surrounding the future of calving events (Larsen *et al.* 2015).

Mendenhall Glacier mass loss

Mendenhall Glacier is a temperate maritime lake-terminating glacier with a sustained floating terminus that is experiencing rapid ice loss through ablation and calving events. Temperate glaciers are especially sensitive to climate, and Mendenhall Glacier's geographic and climatic location leaves it susceptible to large quantities of winter seasonal snowfall but also high rates of summer seasonal melt. The glacier terminus has retreated over 3 kilometers since the start of the 20th century, and the lower extent of the glacier has thinned in excess of 200 meters since the first topographic map was created in 1909. This decline in glacial health can be attributed primarily to surface ablation and secondarily to calving events, though the latter is only responsible for roughly 6% of total ice loss (Motyka *et al.* 2002).

Lake-terminating glaciers in coastal regions are experiencing more rapid terminus thinning and more negative mass balances where well-developed proglacial lakes formed (Larsen *et al.* 2015). Proglacial lakes form at the terminus of a retreating glacier as meltwater fills areas of glacial erosion. These proglacial lakes then modify glacial behavior by increasing calving events and accelerating retreat through overdeepening along the glacial bed near the terminus. This change in glacial bed geometry creates dynamic instabilities, which can cause calving events at a scale similar to that of a tidewater terminating glacier (Larsen *et al.* 2015; Boyce *et al.* 2007; Motyka *et al.* 2002).

The proglacial Mendenhall Lake began to form in the early 1930s. Boyce *et al.* (2007) chose to study terminus dynamics of Mendenhall Glacier because it provides an ideal example for analyzing calving rate as related to a buoyancy-driven mechanism in which ice thickness and water depth control the position of the glacial terminus. An 80–90-meter-deep basin beneath the eastern side of the terminus was determined to be the location of the most significant changes to

the terminus geometry, which is corroborated by this study's observations via satellite imagery (Boyce *et al.* 2007).

Terminus flotation on a proglacial lake can be relatively stable under perfect conditions, but the average annual air temperature at Mendenhall Glacier has increased approximately 1.6 degrees Celsius since 1943, changing melt pattern characteristics (Boyce *et al.* 2007; Motyka *et al.* 2002). Mechanics of lake-calving glacier stability were extensively studied at Mendenhall Glacier by Boyce *et al.* (2007) and were described in a chronological pattern: 1) terminus ice thinning by ablation; 2) ice flotation and upwarping of the glacier terminus; 3) instability of the terminus; 4) short timescale proglacial water-level rise, attributed to summer melt or precipitation events and; 5) remaining terminus stability overcome to produce calving occurrences.

The process of glacier terminus thinning by ablation is increasing due to warming regional climates, meaning the foundational step for calving events is getting more common. Although total ice mass loss at Mendenhall Glacier is not substantially due to calving, calving events play a large role in terminus dynamics and therefore affect the movement of glacial ice. If current polar summer warming trends continue, the thinning and retreat rates of Mendenhall Glacier attributed to increased ablation and calving events will continue to be high and will increase ice mass loss.

CHAPTER III

LITERATURE REVIEW

This section provides an introduction to previous research in the realm of climate-glacier interactions and also reviews methodologies executed in studies of glacial movement over time. This review has two overarching goals: 1) provide context for the current state of the science in terms of climatic forcings on glacial health and 2) present previously implemented methodologies utilized in examining glacial movement with respect to interannual glacial stability on regional and global spatial scales. The review comprehensively considers published findings of glacial movement with respect to anthropogenically-induced climate change.

Evidence of atmospheric oscillation influence on glacial mass-balance

Atmospheric circulation patterns influence seasonal precipitation development, precipitation type, wind velocity and direction, and temperature. These global oscillations have regional effects on ice sheets and glaciers that vary depending on their location. For example, there is an observed positive feedback on winter mass accumulation on Scandinavian glaciers from the October-May Arctic Oscillation (AO) and the October-May North Atlantic Oscillation (NAO). Rasmussen and Conway (2005) used daily upper-air values to analyze 10 glaciers in Norway and two in Sweden, finding that all 12 glaciers exhibited a positive correlation between winter mass balance and both the AO and NAO. An increase in winter mass-balance following 1988 is credited to an increase in precipitation caused by an atmospheric circulation shift to more westerly flow from an easterly flow, resulting in temperatures approximately 2.5 degrees Celsius warmer (Rasmussen and Conway 2005).

While western North American continental glaciers are primarily affected by mesoscale factors, western North American coastal glaciers' winter mass-balances are heavily influenced by North Pacific meteorological conditions and decadal climatic patterns of the Arctic Oscillation (AO), the El Niño-Southern Oscillation (ENSO), and the Pacific Decadal Oscillation (PDO). Many studies observe an increase in glacial mass loss. From 1989–1995, Hodge *et al.* (1998) recorded unprecedented net mass loss at three glaciers, one in the Pacific Northwest and two in Alaska. Menounos *et al.* (2019) noted that western North American glaciers outside of Alaska experienced a fourfold increase in mass loss over the period 2009 to 2018 as compared to 2000–2009. These increases are attributed to changes in regional weather conditions due to the weakening and a spatial shift of upper-level zonal winds.

The AO, ENSO, and PDO all appear in the literature to affect individual glaciers differently, reducing synoptic scale trends to microclimate effects. For example, the PDO has been linked to southeastern Alaskan glacial mass balances, but in a similar fashion to the AO and ENSO, effects are glacier specific. Local variations prevent larger-scale conclusions, as some regions will experience drought while others receive high quantities of precipitation during a phase of the PDO or ENSO, and vice versa. However, regional mean annual temperatures appear to be dependent on the phase of the PDO. Neal *et al.* (2002) observed that southeast Alaskan temperatures were higher during a warm phase of the PDO than during the previous cold phase. For example, the average annual temperatures for Juneau were 5.6 degrees Celsius during the warm phase and 4.3 degrees Celsius during the cold phase. The winter seasonal temperature mean during the warm phase was 2 degrees Celsius warmer, contributing to a decrease in snowfall by 35% as compared to the cold phase (Neal *et al.* 2002). There is a dearth of literature extensively examining the long-term influences of atmospheric oscillation patterns

on glacial mass-balance, but what is available suggests that upper-level shifts affect regional meteorological factors attributed to annual glacial growth and retreat on a localized scale. Previously implemented methodologies for glacial study

Glacial research began well over a century ago with the creation of topographic maps from field-based expeditions, but efficient and reliable quantitative data collection did not begin until the 1970s with the availability of satellite imagery, particularly the 80 square meter resolution Landsat Multi Spectral Scanner (MSS) and the subsequent 30 square meter Landsat Thematic Mapper (TM) sensor the following decade (Paul *et al.* 2015). Satellite sensors provide data on glacier characteristics that are challenging to monitor via ground-based field measurement because these areas are often remote and extremely difficult to access. Optical satellite sensors can measure glacier area and elevation change, and optical microwave satellite sensors can calculate surface ice velocities (Paul *et al.* 2015). Satellite radar interferometry using short orbital and temporal lapses between successive satellite passes captures rapid ice movements of glaciers, and interferometric maps also reveal fringe patterns and assist in the development of quantitative dynamic models (Massonnet and Feigl 1998).

Remote sensing used for glacial health analysis

The efficiency of glacial health data collection has improved dramatically in the last fifty years. Aerial photography and field measurement were once considered extreme methodologies. In contemporary studies, they are the norm. Where airplanes were used to collect aerial photography, now unmanned aircraft systems (UAS), incorporating unmanned aerial vehicles (UAVs) and ground control points, are used in their place. UAS provide more reliable and precise data and more extensive coverage while requiring fewer researchers in the field and reducing emissions from airplanes. With the development of new forms of satellite and remote

sensing imagery analysis techniques, the ability to monitor glacial change has become more practical in terms of time and monetary costs.

Digital elevation models (DEMs) derived from spaceborne satellite imagery or airborne stereo image data are useful in calculating glacial volumetric changes, which is notoriously challenging. From DEM data, geomorphometric models of topographic controls can be developed to assist in analysis of glacial mapping, elevation change, and glacial mass-balance (Quincey *et al.* 2014). Menounos *et al.* (2019) utilized 15,000+ multisensory DEMs generated from the Advanced Spaceborne Thermal Emission and Reflection Radiometer (ASTER) visible and near infrared instrument, which provided spaceborne satellite imagery for assessment of snowpack and glacier mass change. Similarly, Melkonian *et al.* (2014) stacked DEMs from ASTER and the Shuttle Radar Topography Mission (SRTM) to calculate elevation change rates of the Juneau Icefield with a goal of quantifying the icefield's contribution to sea-level rise. In the process, the authors produced the first-ever high-resolution map of ice velocities for Juneau Icefield (Melkonian *et al.* 2014).

The geodetic method implements remote sensing techniques alongside traditional surveying and has a variety of geoscientific applications. Lambrou and Pantazis (2006) generated a 3d Digital Terrain Model of the rocky cliffs surrounding the Monemvasia fortress in Greece with an accuracy of approximately ± 2 cm. The accuracy and resolution capable via the geodetic method allows for clear determination of the topographic surface, including specific rock borders, empty spaces between rocks, and crevices or crevasses (Lambrou and Pantazis 2006). Cox and March (2004) applied the geodetic method to Gulkana Glacier, Alaska. DEMs were created for 1974, 1993, and 1999 using aerial photography to calculate the geodetic balances, and their results showed the thinning rate of glacial ice mass tripled in the 1990s.

Applications of the geodetic method in glacial study are ideal for interannual or decadal mass-balance measurements. Differencing surveyed elevations and adjusting for glacial density can provide measurement of glacier-wide mass-balance between the DEMs (Cox and March 2004).

Remote sensing is a rapidly advancing method for geoscientific study with broad applications to glacial research. As analysis techniques evolve and spatial resolution of satellite or UAS captured images improves, the accuracy of mass-balance measurements will be enhanced. Additionally, measurements of glacial ice volume and ice velocity will become easier to accomplish and more accurate, opening the door for extensive study of dynamic glacier behavior.

Historical use of repeat photography

Repeat ground-based photography is commonly used to document and monitor spatial and temporal environmental changes. In geographic sciences, it is most often used for geomorphological analysis and can be performed on any temporal scale, ranging from 5-year studies to century-long studies implementing historical photograph comparisons to contemporary imagery. Hayes *et al.* (1976) implemented repeat photography to monitor change to the geomorphology of the southern Alaskan coast, particularly how glacial movement, earthquake activity, and strong extratropical cyclones affect the five different categories of glacial outwash plain found in the region as described in Chapter 2. The results of repeat photography from 1969 to 1975 provided Hayes *et al.* (1976) with clear indication of how these dynamic mechanisms affect each category. Regional retreating coasts were seen to be eroding rapidly, increasing the mass of unstable sediment buildup in the prograding spits. Actively eroding glacial margins and glacial outwash coasts are eroding and highly variable. Abandoned glacial coasts did not show

significant change in the series of photographs, which the authors attributed to minimal wave disturbance (Hayes *et al.* 1976).

Prior to the common adoption of Geographic Information System (GIS) technologies, the practice of quantifying repeat photography was accomplished through contour lines. Butler and DeChano (2001) provide an example of this analysis technique in their study of environmental change in Glacier National Park, Montana. Their study sourced 360° panoramic photographs taken from fire lookouts in the 1930s and compared them to the authors' 360° panoramic photographs taken between 1998 and 2000. The authors were looking for notable landscape change, and the results of analysis included dramatic glacial retreat, infilling of snow-avalanche paths, forest succession, and an upward advance of the treeline.

Following initial qualitative analysis, Butler and DeChano (2001) compared the historical photographs to a 1:24,000-scale topographic map with 40 ft contour line intervals to determine the scale of the images. Regions that had been subject to change were outlined, and the dimensions were calculated and compared back to the contour lines on the map. The same was performed on the contemporary photographs, ensuring the same spatial scale was maintained. With area dimensions ready for comparison, percent change was then calculated (Butler and DeChano 2001).

The most efficient, current method of repeat photography analysis is pixel-to-pixel raster data analysis through GIS software programs. For example, Hendrick and Copenheaver (2009) detailed this method in their study of vegetation changes in rural Appalachia. These authors paired historical photographs with contemporary photographs to demonstrate land use change and predict how these areas may respond in the future to anthropogenic climate change and/or

urban or agricultural development. More importantly to this review, the authors outlined, step-by-step, the current common practice of pixel-to-pixel calculations.

After identifying suitable historical images, contemporary photographs were taken while maintaining the same landscape features, camera angle, and field of view. Photographs were then imported into the authors' software of choice and cropped to the same pixel resolution with matching frame extent. Pixels were then categorized by land type, sky, vegetation, etc. to be counted for each photograph. Pixel counts were then used for percent change calculations over time (Hendrick and Copenheaver 2009). This is the most current method of analyzing repeat photography, and as resolution of digital images improves there will be an increase in the amount of detail that this method of study will be able to produce.

Photographic evidence of decadal changes in glacial movement

Historical repeat photography remains applicable to glacial health studies due to the nature of decadal temporal scales at which glacier movement trends occur. Annual variability of glacial movement is subject to many minute meteorological and climatic factors, but decadal trends can be identified through repeat imagery analysis and multi-year measurement. Previous glacial repeat photography studies observe Arctic glacial retreat (Nolan *et al.* 2005; Rapp 1996; Field 1947). Kärkerieppe Glacier in northern Sweden has been melting and retreating, indicated through photographic comparisons between 1907, 1992, and 1995 (Rapp 1996). Ekman Glacier in northern Sweden produced Lake Ekman via retreat in the 1950s. The lake was at its widest point in 1958, but extreme snow accumulation from 1991–1992 led to a period of 50-meter glacial advancement into the lake in 1993. This is shown in photographic analyses from 1985 and 1993 (Rapp 1996).

Nolan *et al.* (2005), using airborne laser altimetry longitudinal profiles corroborated by ground-based surveys alongside photographic comparisons between 1958 and 2003, found McCall Glacier, Alaska, experienced an increase in average thinning rates from 1958–2002. Historical repeat photography of Glacier Bay National Park, Alaska, dates back to 1880 with the first available photograph of Muir Inlet by G.D. Hazard (National Park Service 2017). In 1947, Muir Inlet of Glacier Bay, Alaska, exhibited the most retreat of any observable glacier at the time. Field (1947) took field measurements and compared historical maps and photographs, determining that in the prior ~70 years land cover by glaciers decreased by 175 square miles (35%) and exposed areas of sea increased 47 square miles. Now separated into 12 smaller glaciers due to glacial retreat, Muir Glacier was a single large entity in the 1890s (Field 1947).

Repeat photography has most commonly been utilized in mountainous regions where terrain features are easier to establish between photographs (Hendrick and Copenheaver 2009; Butler and DeChano 2001). Repeat photographs serve as an important data source for glacial study, and this method has the potential to be used more extensively in collaboration with other forms of analysis, such as satellite imagery analysis and climate trend analysis, to provide a more comprehensive view of a glacier or region's story. As Hendrick and Copenheaver (2009, pg. 21) wrote, "When combined with other historical land use methods, repeat photography can yield a detailed reconstruction of the historical profile of an area." There is a lack of glacial research implementing a combined methodological strategy such as this, but with continuing improvements in technology and analysis techniques, it will become more feasible.

CHAPTER IV

DATA AND METHODS

Outlined in this chapter is the process that was followed for data collection, organization, and analysis. This study took a cumulative approach to quantitative analysis of a variety of data sources. The study's methodology is discussed first by individual data preparation and manipulation followed by correlation analyses of the different variables.

Data collection and organization

Data for this study include atmospheric oscillation data, weather data, sea surface temperature data, and Landsat satellite imagery. The temporal scale begins in 1970 and continues through the end of the summer melt period of 2018. The glacial summer melt period consists of the months of June, July, and August. This period is referred to as Summer N throughout. Annual scale in the context of this study is defined as 01 September to 31 August of the following year. For example, Study Year 1 is 01 September 1970 through 31 August 1971 and includes Summer 1 (Table 1).

Oscillation data

Monthly oscillation index data were downloaded from the National Oceanic and Atmospheric Administration (NOAA) for the Arctic Oscillation, the Southern Oscillation, and the Pacific Decadal Oscillation (NOAA/NCDC 2021a; NOAA/NCDC 2021b; NOAA/NCDC 2021c). Negative index values for the Arctic Oscillation (AO) indicate a negative phase, which is associated with warmer temperatures and increased ice melt potential. The Southern Oscillation Index (SOI) is indicative of El Niño and La Niña phases of the El Niño Southern Oscillation. Positive index values represent cool ocean waters (La Niña phase), and negative

Table 1. Study Year dates. This table provides the date range for each Study Year (SY).

Study Year	Date Range	SY	Date Range
1	01 September 1970 - 31 August 1971	25	01 September 1994 - 31 August 1995
2	01 September 1971 - 31 August 1972	26	01 September 1995 - 31 August 1996
3	01 September 1972 - 31 August 1973	27	01 September 1996 - 31 August 1997
4	01 September 1973 - 31 August 1974	28	01 September 1997 - 31 August 1998
5	01 September 1974 - 31 August 1975	29	01 September 1998 - 31 August 1999
6	01 September 1975 - 31 August 1976	30	01 September 1999 - 31 August 2000
7	01 September 1976 - 31 August 1977	31	01 September 2000 - 31 August 2001
8	01 September 1977 - 31 August 1978	32	01 September 2001 - 31 August 2002
9	01 September 1978 - 31 August 1979	33	01 September 2002 - 31 August 2003
10	01 September 1979 - 31 August 1980	34	01 September 2003 - 31 August 2004
11	01 September 1980 - 31 August 1981	35	01 September 2004 - 31 August 2005
12	01 September 1981 - 31 August 1982	36	01 September 2005 - 31 August 2006
13	01 September 1982 - 31 August 1983	37	01 September 2006 - 31 August 2007
14	01 September 1983 - 31 August 1984	38	01 September 2007 - 31 August 2008
15	01 September 1984 - 31 August 1985	39	01 September 2008 - 31 August 2009
16	01 September 1985 - 31 August 1986	40	01 September 2009 - 31 August 2010
17	01 September 1986 - 31 August 1987	41	01 September 2010 - 31 August 2011
18	01 September 1987 - 31 August 1988	42	01 September 2011 - 31 August 2012
19	01 September 1988 - 31 August 1989	43	01 September 2012 - 31 August 2013
20	01 September 1989 - 31 August 1990	44	01 September 2013 - 31 August 2014
21	01 September 1990 - 31 August 1991	45	01 September 2014 - 31 August 2015
22	01 September 1991 - 31 August 1992	46	01 September 2015 - 31 August 2016
23	01 September 1992 - 31 August 1993	47	01 September 2016 - 31 August 2017
24	01 September 1993 - 31 August 1994	48	01 September 2017 - 31 August 2018

index values represent warm ocean waters (El Niño phase). A positive polarity in the Pacific Decadal Oscillation (PDO) index represents a warm phase of the PDO, which is associated with warm sea surface temperatures along the Pacific Northwest coast, including the Gulf of Alaska. The Southern Oscillation and Pacific Decadal Oscillation have been observed to have similar regional effects on the southeastern Alaskan glacial systems, with their respective warm phases negatively impacting glacier mass-balance by increasing summer melt potential and decreasing

winter ice accumulation (Neal *et al.* 2002). Oscillation data began as monthly index values which were averaged to calculate study year annual means.

Weather station data

Weather data were collected from the station in Auke Bay, Juneau, Alaska (Station ID GHCND:USC00500464; Figure 4; NOAA/NCEI 2021a). This station's dataset has 97% coverage and contains daily precipitation (inches), maximum temperature, and minimum temperature (degrees Fahrenheit) values. Weather data used in analysis were culled to the summer months of June, July, and August for each year. Weather station data were averaged to find monthly means, which were later averaged into summer seasonal means.

Sea surface temperature data

Sea surface temperature (SST) monthly anomalies from 1970 to 2018 were provided by Dr. Lei Meng, downloaded from NOAA (NOAA/NCEI 2021b). SST anomaly data were important for analysis because water temperature can directly affect glacier melt potential as well as influence oscillation impact as previously mentioned. SST anomaly data began as monthly means and were averaged to calculate annual means.

Landsat satellite data

Landsat imagery was available beginning in 1972 from the U.S. Geological Survey (USGS/Earth Resources Observation and Science (EROS) Center 2021a; USGS/Earth Resources Observation and Science (EROS) Center 2021b; USGS/Earth Resources Observation and Science (EROS) Center 2021c; USGS/Earth Resources Observation and Science (EROS) Center 2021d). Therefore, Study Year 1 does not have an image available, and when analyzing these data, as described later in the chapter, Study Year 1 of the climate and SST data is omitted. 1972

was not established as Study Year 1 in order to avoid shortening the temporal scale of all climate data. Satellite images were gathered to represent the glacial area at the end of the summer melt

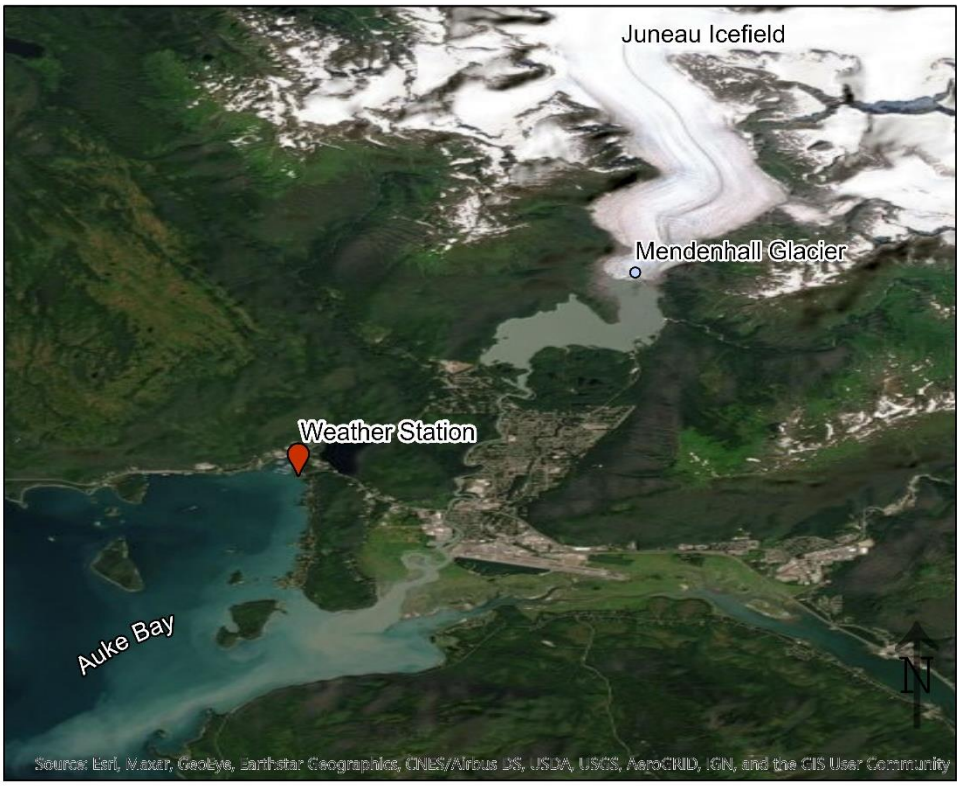

Figure 4. Weather station location. This map shows the location of the Auke Bay weather station relative to Mendenhall Glacier.

period of the respective study year, meaning that the date of the image acquisition may fall into the date range of the following study year.

To collect the satellite imagery, a filter was implemented on the USGS Earth Explorer website for 0-50% cloud cover, and the months of August and September for each year were selected. The ideal date range for image acquisition was initially set from 25 August to 30 September to allow for the changing dates of satellite passing with a goal date around the beginning of September. The initial search did not yield a useable image for all study years within the ideal date range. The cloud cover filter was removed and the search dates expanded into early August in order to obtain useable images for the remaining years of the study. Table 2

provides the image acquisition date for each study year, the satellite, and the sensor responsible for the image.

Table 2. Satellite image details. This table contains details for the Landsat (L) satellite images used in glacier area approximations.

Study Year	Landsat Image Acquisition Date	Satellite	Sensor	SY	Landsat Image Acquisition Date	Satellite	Sensor
1	No Image	N/A	N/A	25	17-Sep-1995	L 5	TM
2	11-Aug-1972	L 1	MSS	26	3-Sep-1996	L 5	TM
3	11-Sep-1973	L 1	MSS	27	13-Sep-1997	L 5	TM
4	6-Sep-1974	L 1	MSS	28	16-Sep-1998	L 5	TM
5	14-Aug-1975	L 1	MSS	29	28-Sep-1999	L 5	TM
6	16-Aug-1976	L 2	MSS	30	28-Aug-2000	L 7	ETM
7	17-Sep-1977	L 2	MSS	31	9-Sep-2001	L 7	ETM
8	16-Aug-1978	L 3	MSS	32	3-Sep-2002	L 7	ETM
9	7-Sep-1979	L 2	MSS	33	23-Sep-2003	L 5	TM
10	5-Aug-1980	L 3	MSS	34	8-Sep-2004	L 7	ETM
11	26-Aug-1981	L 2	MSS	35	11-Aug-2005	L 5	TM
12	20-Aug-1982	L 4	MSS	36	14-Sep-2006	L 7	ETM
13	8-Sep-1983	L 4	MSS	37	2-Sep-2007	L 5	TM
14	25-Sep-1984	L 5	TM	38	19-Aug-2008	L 5	TM
15	5-Sep-1985	L 5	TM	39	14-Sep-2009	L 5	TM
16	15-Sep-1986	L 5	TM	40	18-Sep-2010	L 7	ETM
17	10-Aug-1987	L 5	TM	41	11-Jul-2011	L 5	TM
18	2-Jul-1988	L 5	TM	42	29-Aug-2012	L 7	ETM
19	16-Sep-1989	L 5	TM	43	2-Sep-2013	L 8	OLI/TIRS
20	25-Aug-1990	L 5	TM	44	20-Aug-2014	L 8	OLI/TIRS
21	28-Aug-1991	L 5	TM	45	8-Sep-2015	L 8	OLI/TIRS
22	30-Aug-1992	L 5	TM	46	1-Sep-2016	L 8	OLI/TIRS
23	11-Sep-1993	L 5	TM	47	20-Sep-2017	L 8	OLI/TIRS
24	12-Jul-1994	L 5	TM	48	16-Sep-2018	L 8	OLI/TIRS

After extracting these satellite image files, a new project was opened in ArcGIS Pro for analysis (ESRI Inc. 2019). Raster bands were then loaded onto a new map plane and labeled for clarity and ease of use. The Composite Bands (Data Management Tool) was utilized to stack three satellite bands into a single raster with Natural Colors visualization. For images utilizing

the Landsat Multispectral Scanner (MSS), the two near infrared bands and the red band were used. For all other sensors, the blue, red, and near infrared bands were used.

Landsat data analysis

A Measure Area inquiry in ArcGIS Pro was performed for automatic calculation of the glacier perimeter and area based on manually plotted vertex points along the edge of the active glacier tongue descending into Mendenhall Lake (Figures 5 and 6; ESRI Inc. 2019). These perimeter and area approximations were reported in square kilometers (sqKm) and square meters (sqM) respectively. Perimeter values were discarded because they were not representative of ice mass loss; they are simply a value based on the changing shape of the glacier. Rate of area change calculations based upon the area approximations were then calculated by hand with Equation 1.

Equation 1:

$$Rate\ of\ Area\ Change = \frac{(Area_{previous\ year} - Area_{current\ year})}{Area_{previous\ year}}$$

Correlation analysis

Correlation analysis was performed utilizing the Microsoft Excel software for all combinations of variables, excluding summer seasonal temperature minimums. Seasonal temperature minimums are not considered in the literature to be a dynamic factor in glacial melt. Calculations were then performed by hand using Equation 2 to determine the t-value for each correlation.

Equation 2:

$$t = r\sqrt{\frac{n-2}{1-r^2}}$$

A confidence threshold of 90% was utilized to determine that the critical t-value ($t_{critical}$) was ± 1.3. This was compared to the calculated t-values to determine correlation significance. To reduce the potential for error, the same equation presented above was then used with $t_{critical}$ to solve for the critical r-value. This correlation coefficient threshold was then compared to those calculated in Microsoft Excel to validate the previous significance testing.

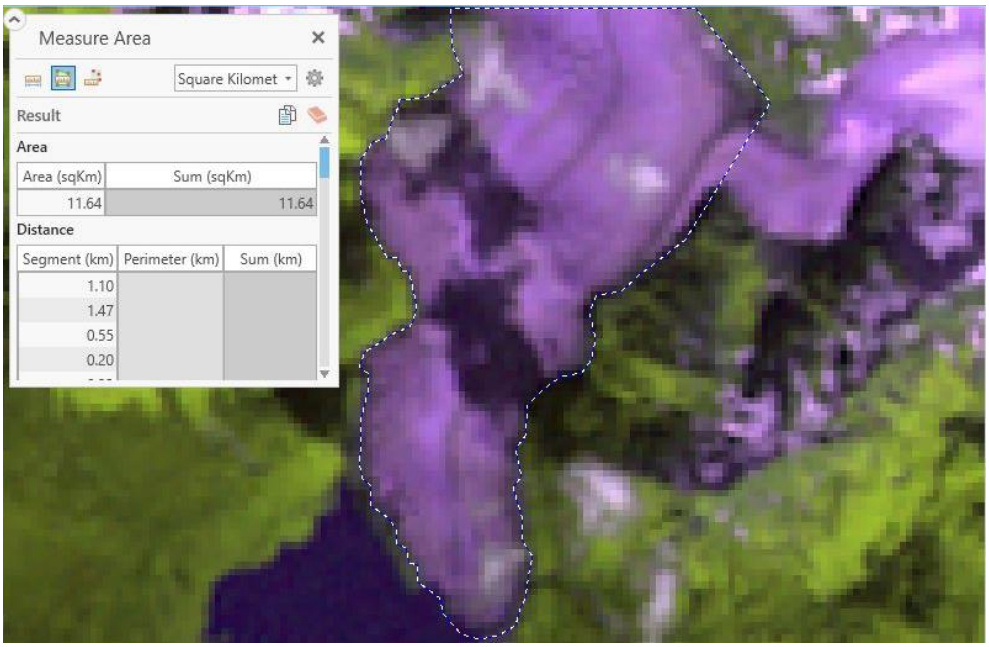

Figure 5. Study Year 2 area. Study Year 2 Landsat image area approximation.

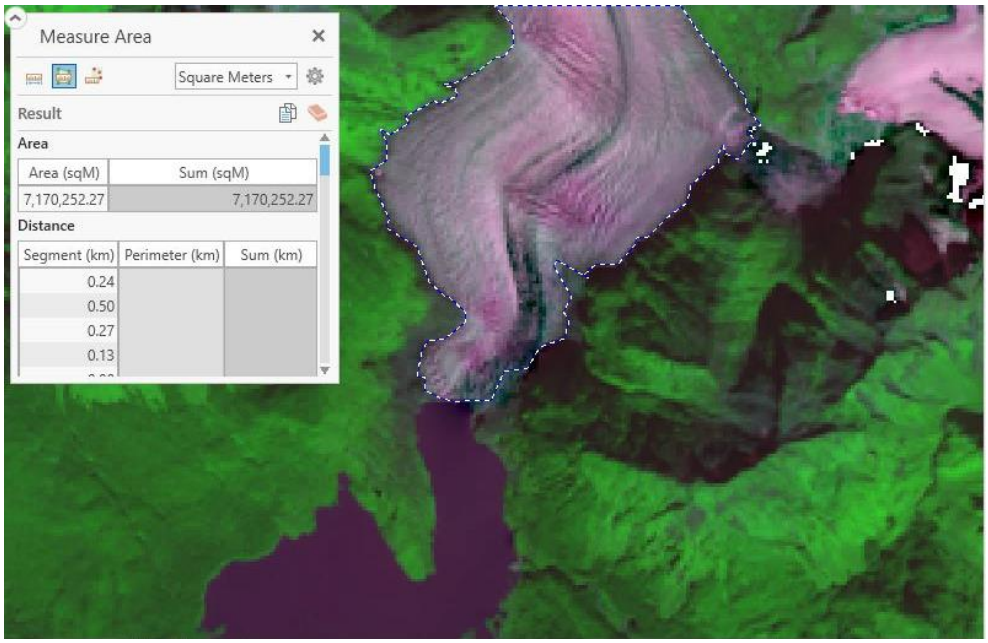

Figure 6. Study Year 48 area. Study Year 48 Landsat image area approximation.

CHAPTER 5

RESULTS AND DISCUSSION

Climate analysis results

Initial analysis of the oscillation data did not indicate any trends. There were an even number of study years in which the Arctic Oscillation (AO) had positive and negative annual index means with no indication of a short-term cyclical nature (Figure 7). There were seven more study years of positive index means for the Southern Oscillation (SOI) than negative index means during the temporal scale of this study, but again no trend can be determined (Figure 8). The Pacific Decadal Oscillation (PDO) demonstrated more negative index annual means, and there appear to be clusters of positive and negative index values (Figure 9). However, no trend is identifiable on this short-term scale. With only a 48-year analysis, long-term trends of these oscillations cannot be definitively determined and only reflect recent natural fluctuations.

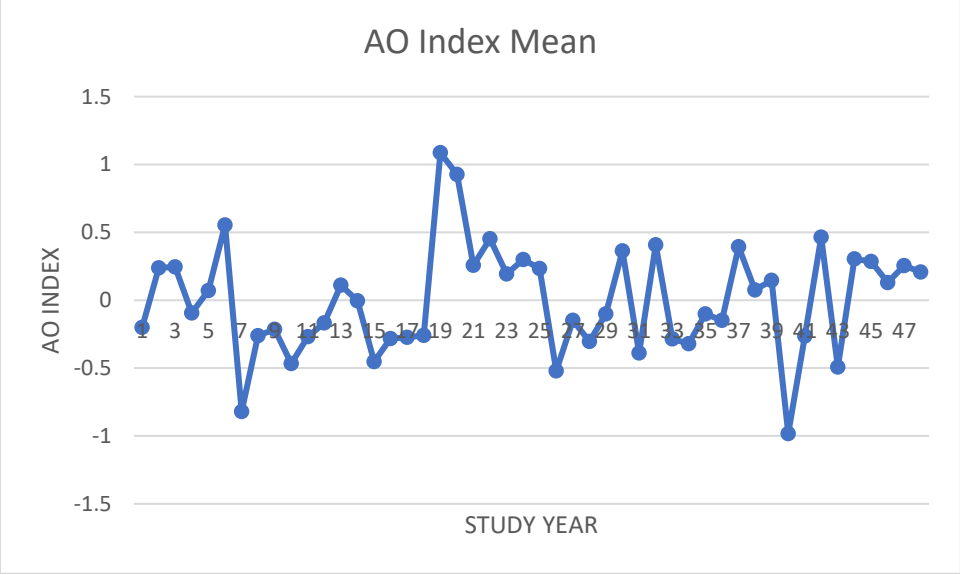

Figure 7. Arctic Oscillation results. This graph depicts the annual mean index values for the Arctic Oscillation.

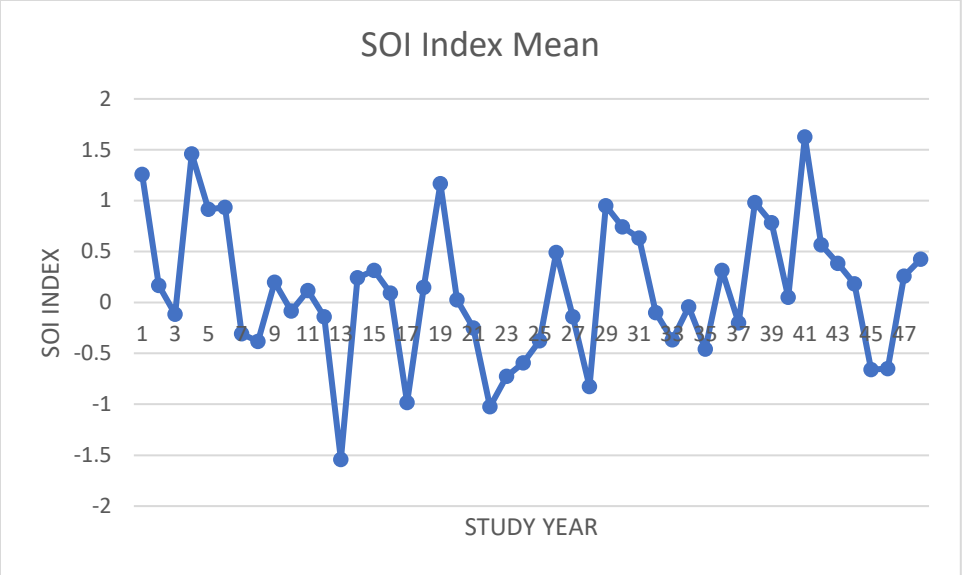

Figure 8. Southern Oscillation results. This graph depicts the annual mean index values for the Southern Oscillation.

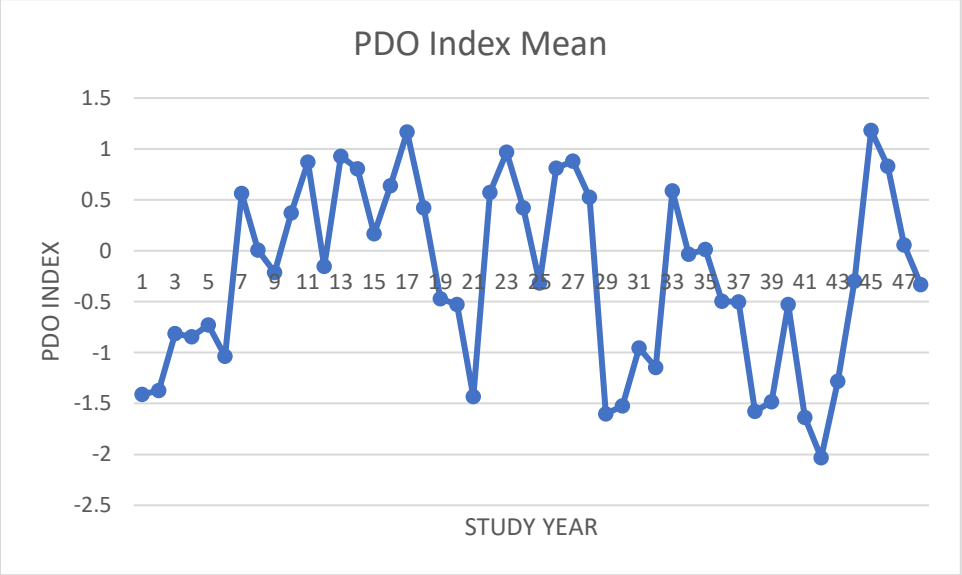

Figure 9. Pacific Decadal Oscillation results. This graph depicts the annual mean index values for the Pacific Decadal Oscillation.

Summer seasonal precipitation means ranged from 0.087 inches to 0.315 inches. There was no identifiable trend in the amount of summer precipitation received, but a plot of the values indicates a possible widening of the range of potential seasonal precipitation (Figure 10).

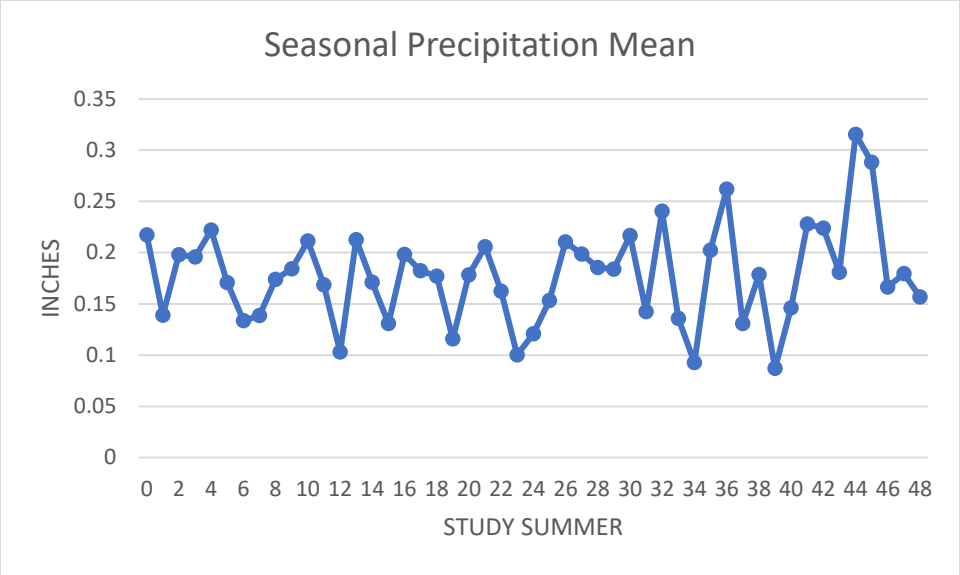

Figure 10. Seasonal precipitation results. This graph depicts the annual mean summer seasonal precipitation totals.

Summer seasonal temperature maximum means ranged from 58.63 degrees Fahrenheit to 69.43 degrees Fahrenheit. No increasing trend was established (Figure 11).

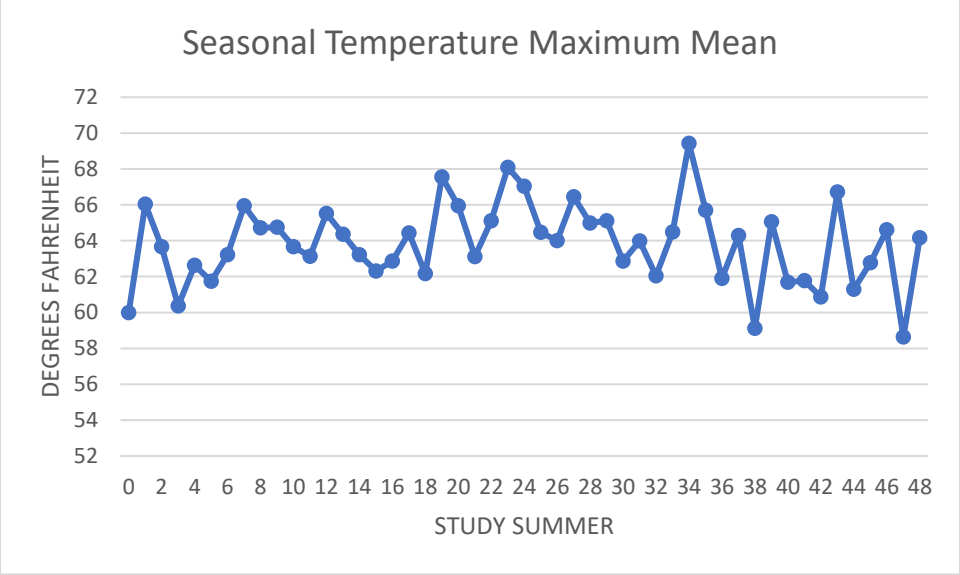

Figure 11. Seasonal temperature maximum results. This graph depicts the annual mean summer seasonal maximum temperatures.

A slight increasing trend can be observed from plotting the summer seasonal temperature minimum means (Figure 12). Temperature minimum means ranged from 45.25 degrees Fahrenheit to 52.66 degrees Fahrenheit.

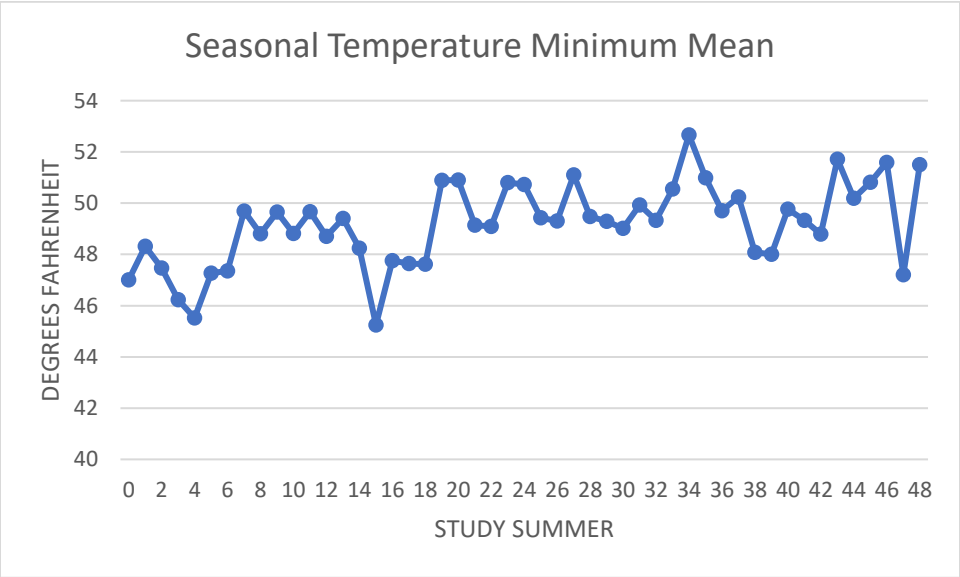

Figure 12. Seasonal temperature minimum results. This graph depicts the annual mean summer seasonal minimum temperatures.

Sea surface temperature (SST) anomaly means range from -1.1668 degrees Celsius to 1.4997 degrees Celsius. The anomalies appear to be demonstrating a slight increasing trend on a slow timescale, but it cannot be a conclusive result with the time frame of this study (Figure 13). An extended climatology is needed to determine a definitive trend. If regional SST anomalies are increasing, glacial health will likely continue to decline as SSTs affect influential climatic variables, such as seasonal precipitation and temperature, which affect both winter growth potential and summer melt potential.

Landsat analysis results

A decreasing trend in glacier area was identified from the area approximations, which corroborates historical photographic imagery comparisons with today's location of the glacier terminus (Figures 1, 2, and 14), but no identifiable increasing or decreasing trend in the

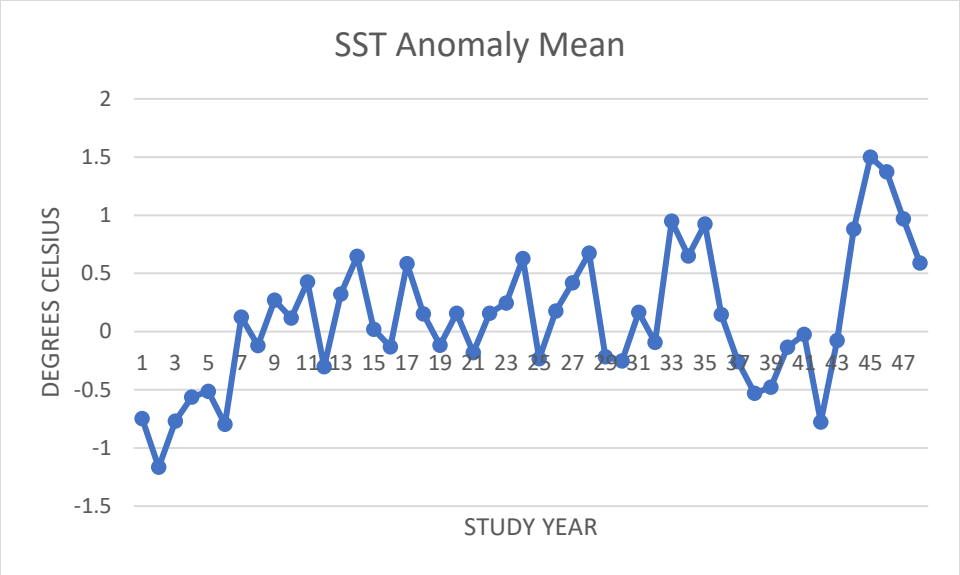

Figure 13. Sea surface temperature anomaly results. This graph depicts the annual mean sea surface temperature anomalies.

rate of area change was calculated (Figure 15). Distinct positive mass-balance years were observed, but they may be the result of numerous factors. Some years may in fact have seen more mass accumulation than mass loss, as noted by Motyka *et al.* (2002) for the growth seen in 2000. There is potential that these growth years received and retained large quantities of snow during the winter season or did not receive the normal budget of summer seasonal insolation, either of which could prevent average annual mass loss. Other years, the perceived growth may be attributed to satellite image quality. During analysis, notes were taken when glacier boundaries were obscured or distorted by clouds, shadow, etc. These images often aligned with the area approximations that resulted in growth, meaning the result is likely a byproduct of analysis error. Simply put, the underlying cause of growth years is left to speculation and needs further study to determine the cause of the results seen here.

It is worth noting that this analysis was based on the top surface area of glacial ice, as volumetric measurements are not feasible without a vertical view of the glacier. The rate of area

change is therefore not synonymous with a rate of total ice loss, which would factor in volumetric change.

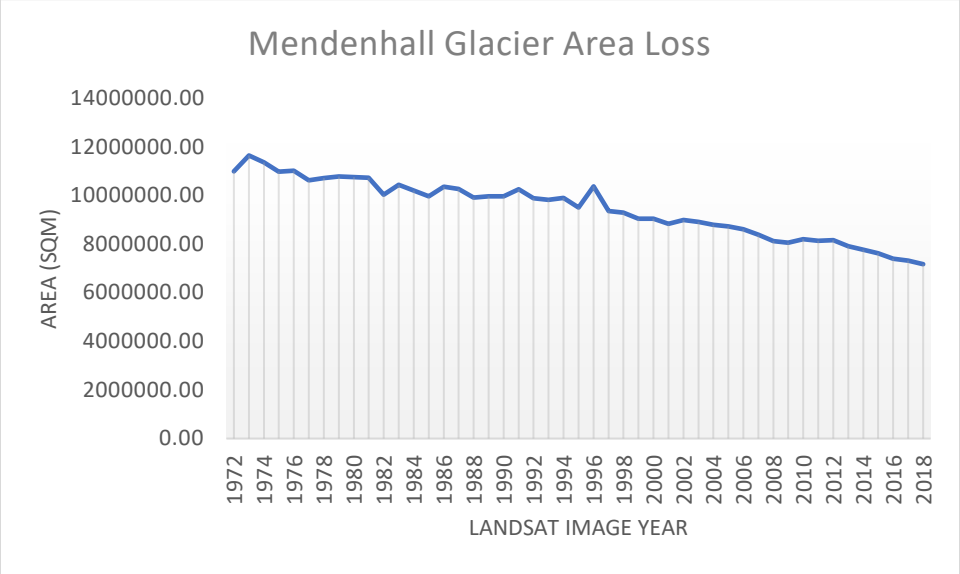

Figure 14. Glacier area loss. This graph depicts the decreasing trend in Mendenhall Glacier ice area approximations.

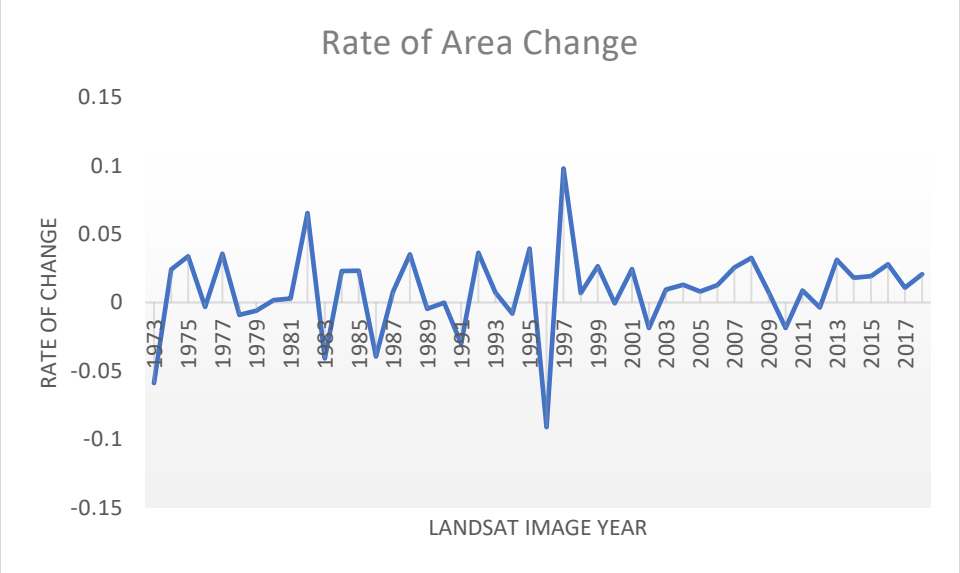

Figure 15. Rate of area change. This graph depicts the calculated interannual rates of area change for Mendenhall Glacier based on the ice area approximations.

Correlation analysis results and discussion

Of the 24 correlations performed, only six were statistically significant (Table 3). Of those, only one is truly relevant to the goal of this study, Mendenhall Glacier ice area loss and sea surface temperature anomalies, which will be discussed last. Each other significant correlation will first be addressed. Why the correlation does not directly apply to this study but may apply in a broader context that needs deeper study will be discussed.

Sea surface temperature anomalies and the Southern Oscillation index

Sea surface temperature (SST) annual mean anomalies and Southern Oscillation (SOI) annual mean index values demonstrated a statistically significant negative correlation, meaning as the SOI index becomes more negative, indicating warmer ocean waters in an El Niño phase, SST anomalies increase (Figure 16). Gulf of Alaska SSTs were not identified to have a distinct increasing trend in the scope of this study, but Bograd et al. (2005) determined that indeed SST anomalies are steadily on the rise, particularly in the northern and eastern portions of the gulf. The SOI particularly impacts the Gulf of Alaska SST anomalies in a meridional fashion, with higher latitudes diminishing the strength of its influence. Studies indicate that at poleward latitudes, the SOI influence is largely restricted to the inshore coastal environment, such as that of Mendenhall Glacier (Bograd *et al.* 2005; Lluch-Cota *et al.* 2001). This result indicates that SOI influence reaches northward into the Gulf of Alaska, and, in a broad context, this could affect the health of Mendenhall Glacier and similar inshore coastal lake-terminating glaciers when negative SOI index values and positive SST anomalies simultaneously favor increased melt potential.

Table 3. Correlation analysis results. This table contains the correlation coefficients for all variable combinations as well as the significance threshold testing. Highlighted rows were calculated to be significant at the 90% confidence level.

Correlation Coefficient (r)	r-critical	Sample Size (n)	Degrees of Freedom (df)	t-critical (t.90)	t-value	Variable Combination
-0.1796	± 0.1923	46	44	± 1.3	-1.2110	Rate and seasonal precip
0.1761	± 0.1923	46	44	± 1.3	1.1866	Rate and seasonal Tmax
0.1313	± 0.1923	46	44	± 1.3	0.8786	Rate and SST Anomaly
-0.0368	± 0.1923	46	44	± 1.3	-0.2444	Rate and AO Index
0.0551	± 0.1923	46	44	± 1.3	0.3664	Rate and SOI Index
0.0287	± 0.1923	46	44	± 1.3	0.1905	Rate and PDO Index
-0.1190	± 0.1903	47	45	± 1.3	-0.8042	Area and seasonal precip
0.1230	± 0.1903	47	45	± 1.3	0.8315	Area and seasonal Tmax
-0.4263	± 0.1903	47	45	± 1.3	-3.1615	Area and SST Anomaly
-0.0550	± 0.1903	47	45	± 1.3	-0.3693	Area and AO Index
-0.0707	± 0.1903	47	45	± 1.3	-0.4756	Area and SOI Index
0.1747	± 0.1903	47	45	± 1.3	1.1904	Area and PDO Index
-0.1078	± 0.1882	48	46	± 1.3	-0.7353	AO and SST Anomaly
-0.5065	± 0.1882	48	46	± 1.3	-3.9846	SOI and SST Anomaly
0.6982	± 0.1882	48	46	± 1.3	6.6148	PDO and SST Anomaly
0.1595	± 0.1882	48	46	± 1.3	1.0956	SST and seasonal precip
0.1703	± 0.1882	48	46	± 1.3	1.1718	SST and seasonal Tmax
0.0693	± 0.1882	48	46	± 1.3	0.4714	AO and seasonal precip
0.0015	± 0.1882	48	46	± 1.3	0.0100	SOI and seasonal precip
-0.0521	± 0.1882	48	46	± 1.3	-0.3535	PDO and seasonal precip
-0.0149	± 0.1882	48	46	± 1.3	-0.1009	AO and seasonal Tmax
-0.2686	± 0.1882	48	46	± 1.3	-1.8910	SOI and seasonal Tmax
0.2690	± 0.1882	48	46	± 1.3	1.8945	PDO and seasonal Tmax
-0.5350	± 0.1863	49	47	± 1.3	-4.3414	S. precip and s. Tmax

Sea surface temperature anomalies and the Pacific Decadal Oscillation index

Sea surface temperature (SST) annual mean anomalies and Pacific Decadal Oscillation (PDO) annual mean index values demonstrated a statistically significant positive correlation, meaning as the PDO index becomes more positive, SST anomalies increase (Figure 17). Northward of 31° N, the PDO takes precedence over the SOI for regional influences, and the PDO index has often been used for monitoring temperature regimes in the Gulf of Alaska region (Bograd *et al.* 2005; Lluch-Cota *et al.* 2001). However, study has shown that the existence of

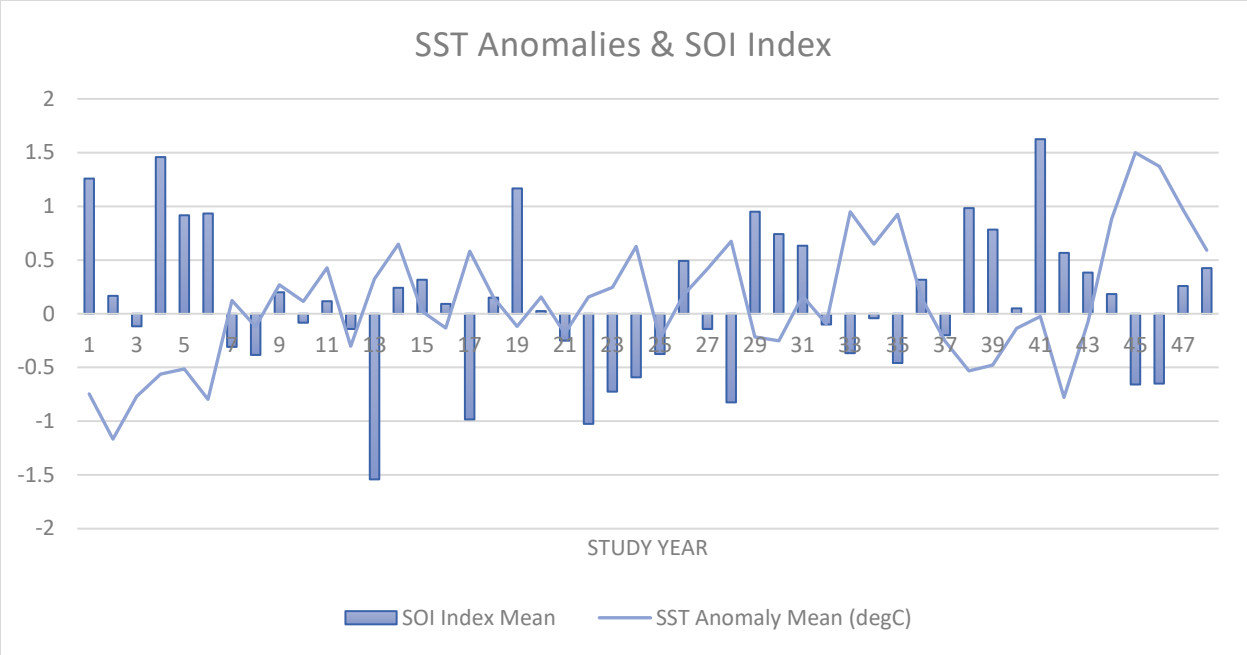

Figure 16. SST anomalies and SOI index correlation. This graph depicts the statistically significant negative correlation between sea surface temperature mean anomalies and the Southern Oscillation mean index values.

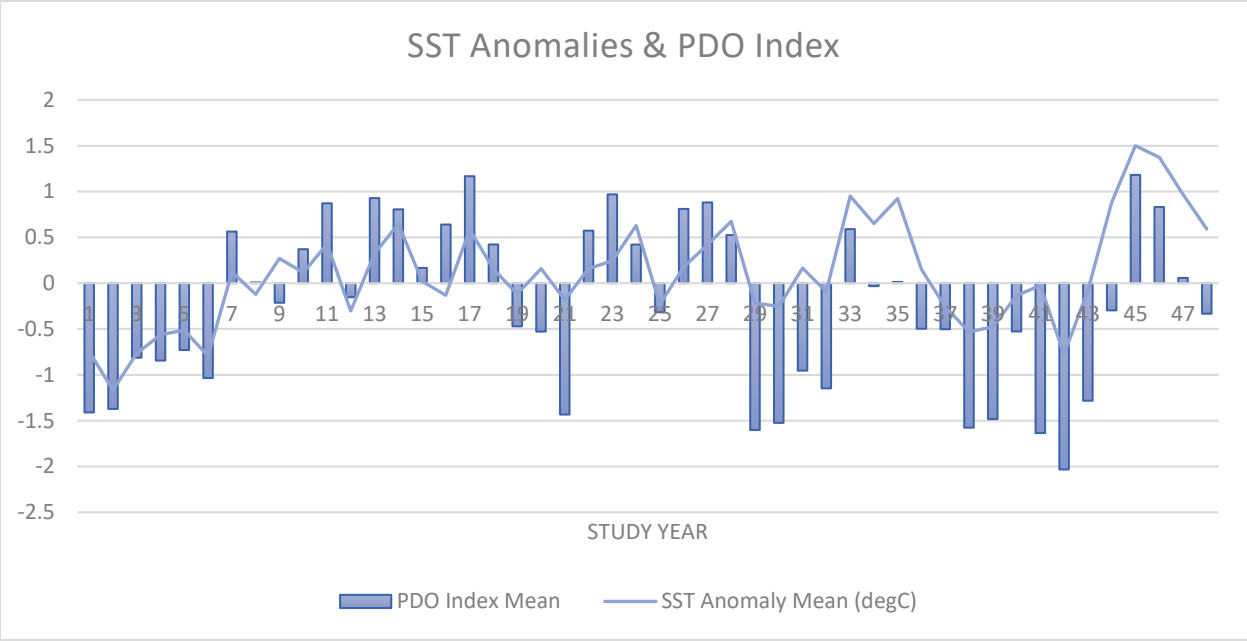

Figure 17. SST anomalies and PDO index correlation. This graph depicts the statistically significant positive correlation between sea surface temperature mean anomalies and the Pacific Decadal Oscillation mean index values.

influence by the both the SOI and PDO in the region obscures their relative contributions to climate variations (Lluch-Cota *et al.* 2001). As the SOI was noted to have stronger effects on inshore coastal environments, the PDO was noted to have stronger effects on oceanic coastal environments at poleward latitudes. The mechanisms that cause the PDO to have weaker influence on inshore coastal environments than on oceanic coastal environments is likely linked to the PDO's movement being directly related to large-scale oceanic processes (Lluch-Cota *et al.* 2001).

Seasonal temperature maximum and the Southern Oscillation index

Summer seasonal mean temperature maximums (Tmax) and Southern Oscillation (SOI) annual mean index values demonstrated a statistically significant negative correlation, meaning as the SOI index becomes more negative, summer Tmax increases (Figure 18). The correlation between the warm phase of the SOI (El Niño phase) and warmer summer temperatures has been well-documented in previous literature, and the SOI's influence on inshore coastal Alaskan regions, such as the location of Mendenhall Glacier, has been noted previously in this discussion (Fleming and Whitfield 2010; Lluch-Cota *et al.* 2001). This direct relationship between the SOI phase and Tmax will subsequently influence glacial melt potential, as temperature maximums are fundamental for mass loss mechanisms.

Seasonal temperature maximum and the Pacific Decadal Oscillation index

Summer seasonal mean temperature maximums (Tmax) and Pacific Decadal Oscillation (PDO) annual mean index values demonstrated a statistically significant positive correlation, meaning as the PDO index becomes more positive, summer Tmax increases (Figure 19). As with the previous result, the warm phase of the PDO has been related to warmer summer temperatures in prior literature (Fleming and Whitfield 2010; Lluch-Cota *et al.* 2001). Likewise,

the direct relationship between the phase of the PDO and Tmax values influences regional melt potential.

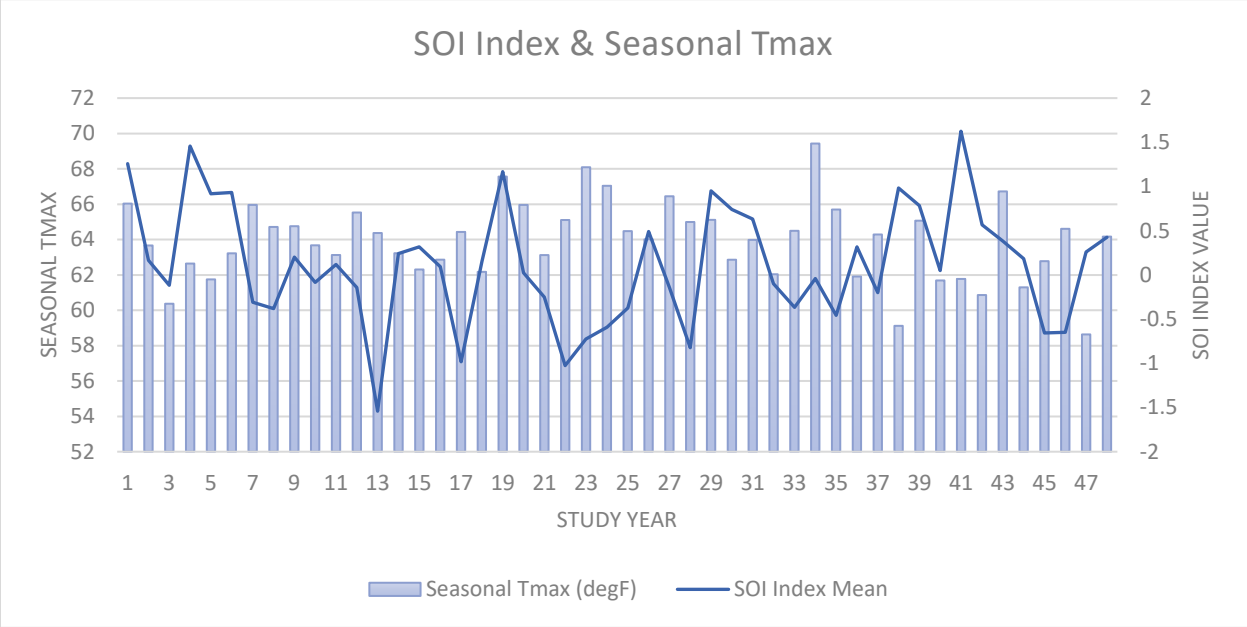

Figure 18. SOI index and seasonal Tmax correlation. This graph depicts the statistically significant negative correlation between summer seasonal mean temperature maximums and the Southern Oscillation mean index values.

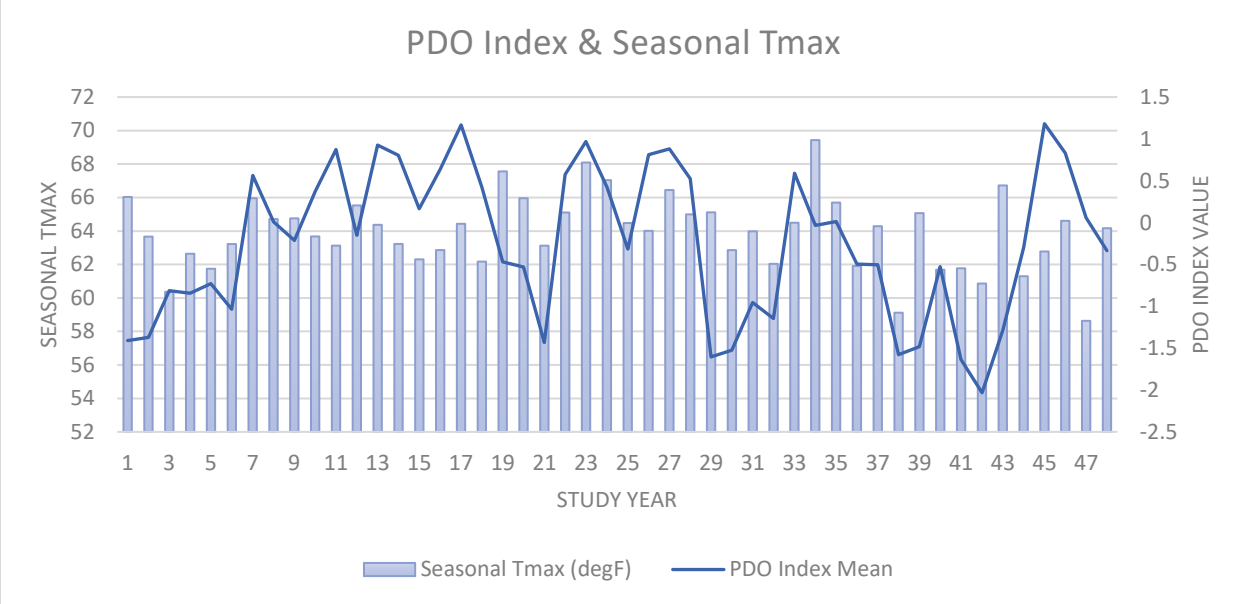

Figure 19. PDO index and seasonal Tmax correlation. This graph depicts the statistically significant positive correlation between summer seasonal mean temperature maximums and the Pacific Decadal Oscillation mean index values.

Seasonal temperature maximum and seasonal precipitation

Summer seasonal mean temperature maximums (Tmax) and summer seasonal mean precipitation (Precip) demonstrated a statistically significant negative correlation (Figure 20). Warmer summer seasonal temperatures were seen during drier conditions, whereas more precipitation was related to cooler temperatures. Warmer, drier conditions are likely to increase mass loss due to the foundational mechanisms that contribute to increased melt potential, but regional characteristics do not always reflect a specific glacier's reaction to climatic conditions. Different combinations of summer seasonal temperature and precipitation create variations between glaciers, particularly in Alaska where glaciers are oftentimes located on topographic divides that serve as transitional climate zones (Larsen *et al.* 2015; Steiner *et al.* 2008). This result demonstrates a correlation based on data in Auke Bay, and though this may be applied regionally, this result by itself may not affect melt potential for Mendenhall Glacier specifically. Only a data collection station located at the glacier itself could provide results without uncertainties surrounding meteorological variable influences.

Sea surface temperature anomalies and Mendenhall Glacier ice area loss

Gulf of Alaska sea surface temperature (SST) anomalies and Mendenhall Glacier area loss demonstrated a significantly negative correlation, meaning higher SST anomalies are linked to less area coverage of glacial extent (Figure 21). This was the only meaningful result that found a direct, significant influence of a variable on ice area loss. Though Mendenhall Glacier is not a tidewater terminating glacier, Gulf of Alaska SST anomalies have a regional effect on the climate regime. Temperature, precipitation, relative humidity, and more climatic variables are all influenced by SSTs. SSTs are also indicative of the Southern Oscillation, which, as discussed previously, has climatic influence over the inshore coastal environments of Southern Alaska.

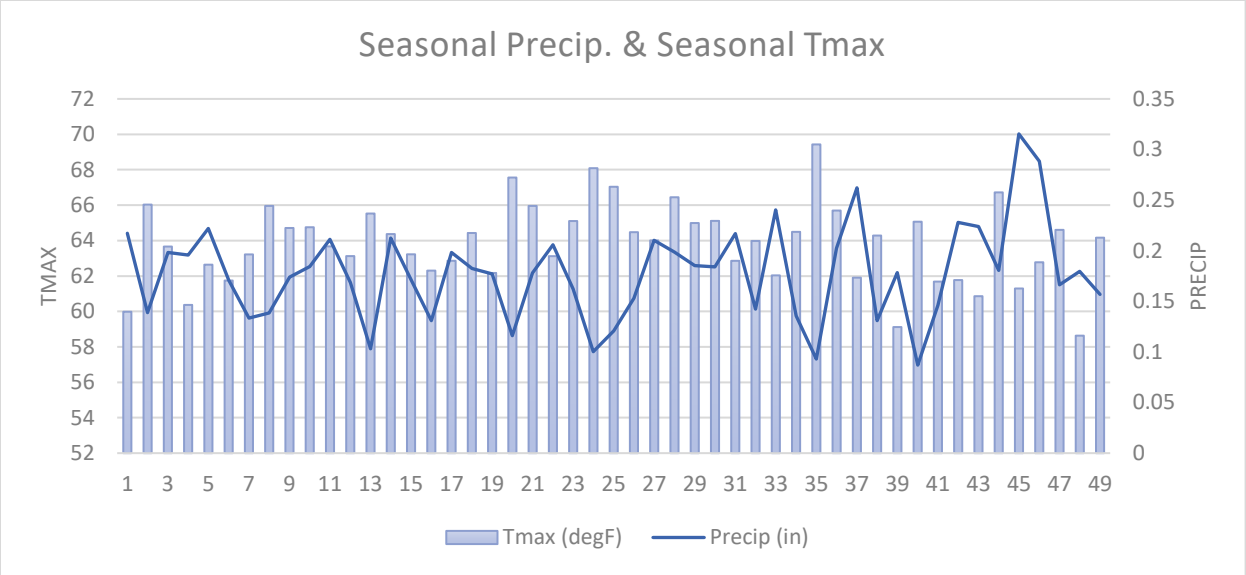

Figure 20. Seasonal Precip. and seasonal Tmax correlation. This graph depicts the statistically significant negative correlation between summer seasonal mean temperature maximums and summer seasonal mean precipitation.

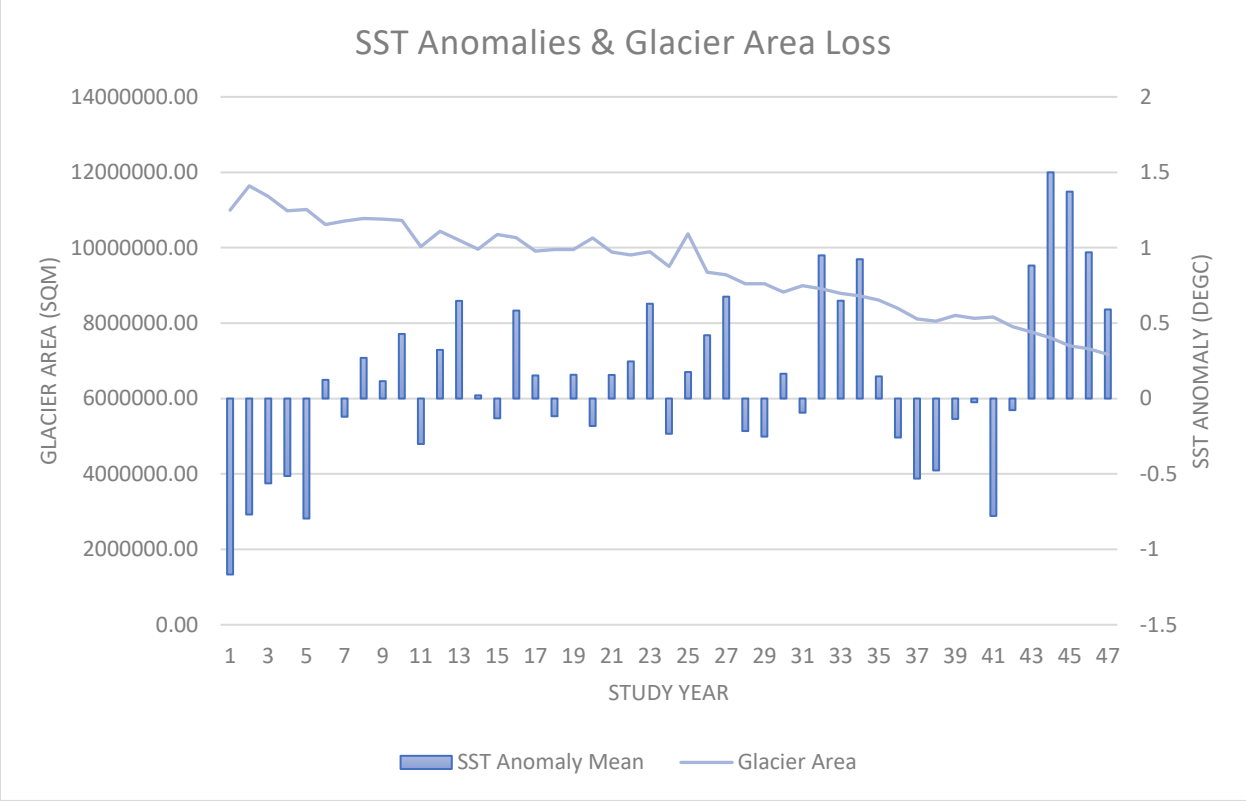

Figure 21. SST anomalies and glacier area loss correlation. This graph depicts the statistically significant negative correlation between sea surface temperature mean anomalies over the Gulf of Alaska and Mendenhall Glacier ice area.

Though direct correlations between summer seasonal precipitation, temperature maximums, or the SOI index and glacier area loss were not significant, the SST anomaly correlation can, in a broad context, relate these variables with ice area loss for the purpose of analyzing melt potential and glacial health influence.

Discussion and implications

Though all data variables were considered in analysis for a broader context, this study addressed six specific research questions, of which one could be answered with an affirmative:

1. Is there a significant correlation between summer seasonal temperature maximum means and glacier area loss? No.
2. Is there a significant correlation between summer seasonal temperature maximum means and the rate of area loss? No.
3. Is there a significant correlation between the Arctic Oscillation, the Southern Oscillation, and/or the Pacific Decadal Oscillation and glacier area loss? No.
4. Is there a significant correlation between the Arctic Oscillation, the Southern Oscillation, and/or the Pacific Decadal Oscillation and the rate of area loss? No.
5. Is there a significant correlation between Gulf of Alaska sea surface temperature anomalies and glacier area loss? Yes.
6. Is there a significant correlation between Gulf of Alaska sea surface temperature anomalies and the rate of area loss? No.

Though summer seasonal temperature maximum (Tmax) means were significantly correlated to the Southern Oscillation (SOI) and the Pacific Decadal Oscillation (PDO), they were not seen to significantly correlate directly with glacier area loss. Tmax is a fundamental factor in the mechanisms that drive glacial mass loss, but regional patterns may not always apply due to the

topographic characteristics of many of Alaska's glaciers, as described above (Larsen *et al.* 2015). However, in a study by Fleming and Whitfield (2010), the seaward side of the Icefield Ranges, where the southeastern Alaskan glacial landscape lies, demonstrated a strong seasonal temperature response as a region to the influence of the SOI and PDO, which differs from the leeward side, the region containing the southwestern Yukon Territory and northwestern British Columbia. The SOI and PDO influences also revealed spatiotemporal patterns in seasonal temperatures that are more uniform than the patterns demonstrated by seasonal precipitation across the southeastern Alaskan coastal region. This is likely a contributing factor in the significant correlations seen in this study and further indicate that they will affect melt potential and glacial health in a broader context.

The lack of a significant correlation between the Arctic Oscillation (AO) and any variable was an unexpected result, as negative phases of the AO have been observed to increase melt potential; however, the AO tends to have its strongest influence on climate during the winter season as compared to the other atmospheric oscillations that affect the region (Dahlman 2009). It is also possible that Mendenhall Glacier is far enough south to be out of range of significant influence by the AO (NSIDC 2020b). Though the SOI and PDO did not correlate to glacier area loss or the rate of area loss, they do correlate to sea surface temperature (SST) anomalies, which in turn did correlate to glacier area loss. The results of this study indicate a stronger correlation between SST anomalies over the Gulf of Alaska and the PDO rather than the SOI. Though the SOI tends to affect inshore coastal environments more strongly than oceanic coastal environments at this latitude, and vice versa for the PDO, the influence of the PDO at this latitude is stronger overall, likely contributing to the SST anomalies.

SST anomalies did not correlate with the rate of area loss, but the rate of area loss itself demonstrated no pattern or trend. SST anomalies did, however, produce a significant correlation with glacier area loss. Though this was discussed in depth earlier in the chapter, it is worth noting a second time that SST anomalies may have an indirect influence on glacial health through the means of other climatic variables, which did not demonstrate significant correlations on their own.

The results confirm Mendenhall Glacier's declining glacial health, but no conclusions can be made regarding which climatic variables have greater influence on glacier area loss. Although this study did not result in conclusive answers to five of the six research questions, it does indicate that SST anomalies play a factor in glacial health, even when the glacier does not terminate directly in ocean waters. Whether this correlation is due to the physical connection of Mendenhall Lake to the Gulf of Alaska via Mendenhall River and a series of coves and bays or is due to SST's regional climatic effects is a subject for further study. The results of this study carry limited regional implications, but there is enough evidence to indicate that other glaciers of the southeastern Alaskan glacial landscape would likely demonstrate a similar correlation to Gulf of Alaska SSTs.

Limitations and room for error

It must be acknowledged that there are strong limitations in the analysis of this study. Due to the COVID-19 pandemic, the fieldwork that was initially planned was not able to be performed. This limited the scope of the study with regard to satellite calibration efforts and current year imagery. There were three holes in the weather dataset. Data were available for solely the month of June in 2009 and 2017 and were available for June and July in 2016. The

seasonal analysis was performed using the June means for 2009 and 2017 and the mean for June and July in 2016.

There are inherent limitations when working with Landsat imagery. Clouds and shadow obscure some glacial boundaries as well as sensor issues with Landsat 7 leaving streaks of no raster data through some images (Figures 22 and 23). Older resolution images are not as clear as Landsat 8 images, meaning that area measurements are by no means exact (Figure 24). It was written as glacier area approximation to account for this. Additionally, not every image used was within the ideal timeframe at the end of the summer melt period. Table 4 isolates these years.

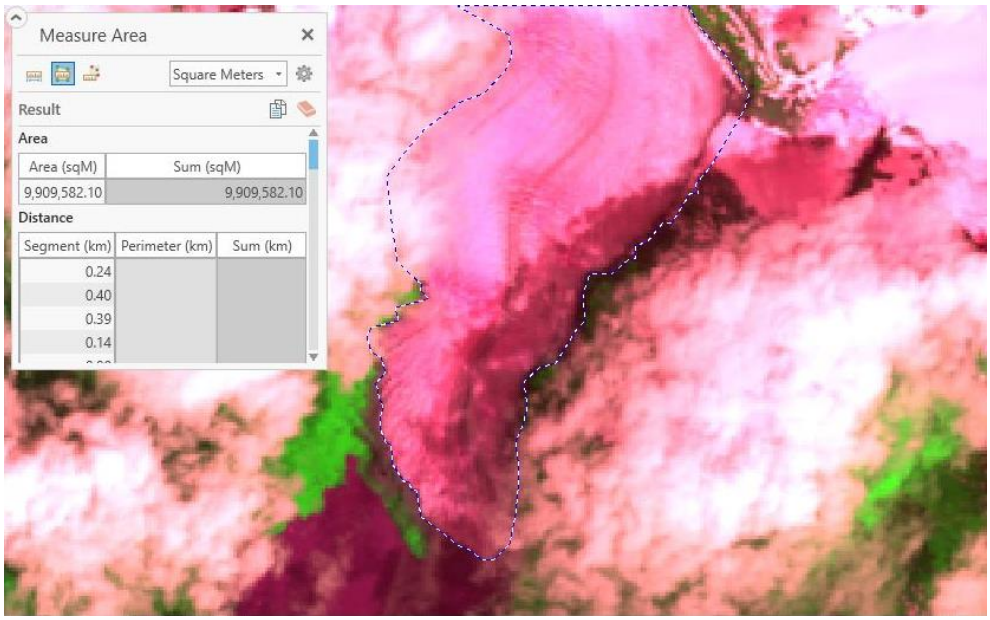

Figure 22. Obscured glacier boundaries. Study Year 18 Landsat image demonstrates an example of clouds and shadow obscuring glacier boundaries.

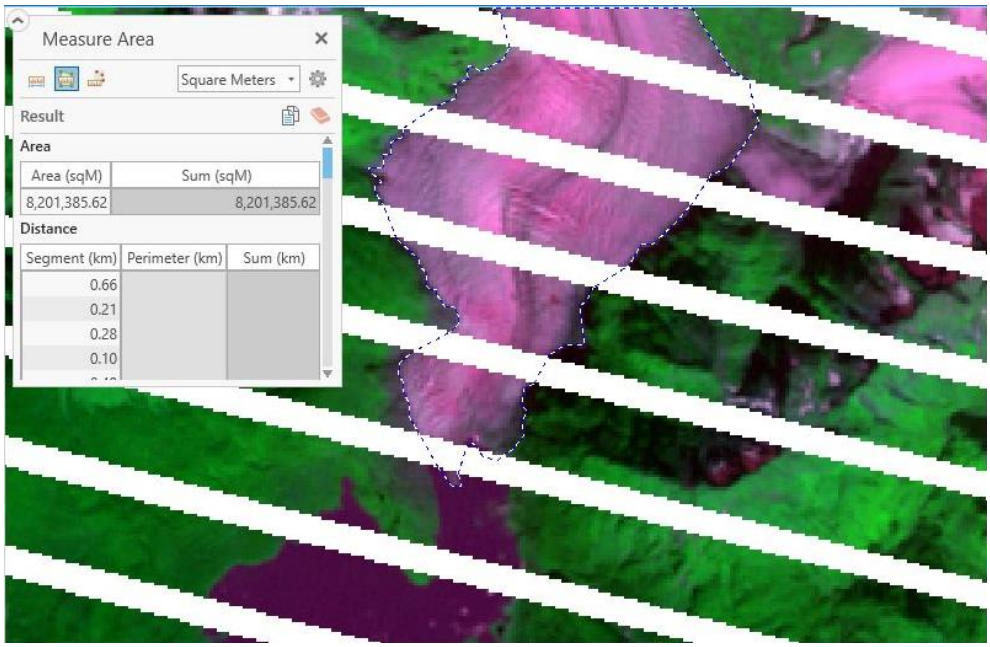

Figure 23. Sensor malfunction image. Study Year 40 Landsat image demonstrates an example of the missing raster data due to a sensor malfunction on the Landsat 7 satellite.

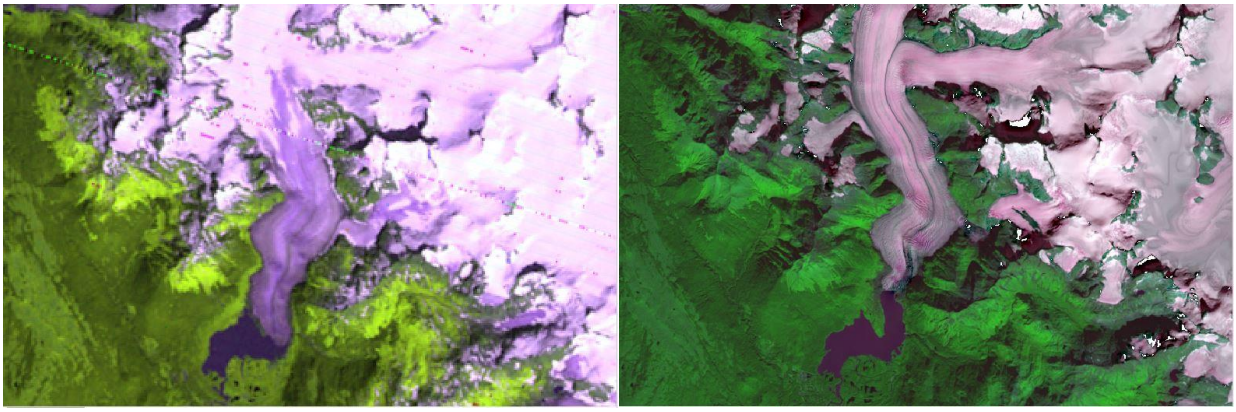

Figure 24. Landsat image clarity comparison. This side-by-side comparison shows the quality difference between a Landsat 1 satellite image from 1972 and a Landsat 8 satellite image from 2018.

Table 4. Landsat images outside ideal timeframe. This table isolates the years of Landsat imagery which were not within the ideal timeframe at the end of the summer melt period (25 August–30 September).

Study Year	Landsat Image Acquisition Date
2	11-Aug-1972
5	14-Aug-1975
6	16-Aug-1976
8	16-Aug-1978
10	5-Aug-1980
12	20-Aug-1982
17	10-Aug-1987
18	2-Jul-1988
24	12-Jul-1994
35	11-Aug-2005
38	19-Aug-2008
41	11-Jul-2011
44	20-Aug-2014

CHAPTER VI

CONCLUSIONS

Mendenhall Glacier is representative of Alaskan lake-terminating glaciers and is demonstrating a clear pattern of interannual retreat. The southeastern shoreline of Alaska is dotted with geomorphologically similar glacial structures, and, when paired with the findings from ample studies in the region, it is apparent that anthropogenically-induced climate change is taking its toll on these ice reserves. The depleting ice volume being driven by glacial melt and frequent calving events will affect freshwater availability, alter the mineral makeup of the soil and water, and contribute to lake- and sea-level rise. Additionally, the changing geometry of glacial boundaries will affect not only glacier terminus stability but also the stability of regional alpine slopes, in which the majority of Alaskan glaciers exist.

This study opens the door for further research at Mendenhall Glacier and across the glacial landscape of the southeastern Alaskan coastline. Improvement upon this study could begin with data expansion. Rather than simply serving as qualitative justification for beginning this study, historical ground photography of the glacier terminus can be quantitatively analyzed via pixel-to-pixel raster analysis and paired with an extended climatology. Extending the regional climatology may uncover long-term trends that were not identified in the 48-year range of this study. Further, an extended climatology would provide the means of analyzing the lagged glacial response to changes in regional climate, and subsequent adjustments to correlation calculations may produce more significant results.

Additionally, less error and more significant results may be produced if analysis were performed for inter-seasonal correlations rather than incorporating off-season means in the

annual timescale. Further, individual summer month analysis could be performed to determine which month produces the most melt on average. Using the resulting month for correlation analysis as performed in this study could be implemented to see if correlations then become significant. Another enhancement to this study would come in the form of a better selection of satellite imagery and an improved analysis technique that could render area calculations rather than rough area approximations. With improved area calculations, the rate of area change may subsequently produce an identifiable trend and/or significant correlations.

Further research could be performed to isolate winter seasonal growth and the interannual growth rate. Winter annual or seasonal correlations have the potential to yield results that indicate less interannual growth, contributing to the decline in glacial health. Additionally, more variables, such as snowfall pattern change, can be analyzed alongside the rate of area change, and there is room to further isolate different dynamic factors of glacial melt, such as melt from underneath the glacier.

Declining glacial health in Alaska seen from the perspective of Mendenhall Glacier is a pressing and current concern within the fields of climatology, glaciology, hydrology, and geomorphology. Further study diving into the complexities of climate-glacier interactions is necessary, as is collaboration between researchers of different scientific backgrounds. Declining glacial health is not a localized problem, but a specific look at Mendenhall Glacier embodies many of the elements contributing to the concurrent issue across Alaska.

REFERENCES

Benn, D.I, C.R. Warren, and R.H. Mottram, 2007: Calving processes and the dynamics of calving glaciers. *Earth-Science Reviews*, **82**, 143–179, DOI:10.1016/j.earscirev.2007.02.002.

Bograd, S.J., R. Mendelssohn, F.B. Schwing, and A.J. Miller, 2005: Spatial heterogeneity of sea surface temperature trends in the Gulf of Alaska. *Atmosphere-Ocean*, **43**, 241–247, DOI:10.3137/ao.430304.

Boyce, E.S., R.J. Motyka, and M. Truffer, 2007: Flotation and retreat of a lake-calving terminus, Mendenhall Glacier, southeast Alaska, USA. *Journal of Glaciology*, **53**, 211–224.

Brocklehurst, S.H., 2013: How glaciers grow. *Nature*, **493**, 173–174, DOI:10.1038/493173a.

Burgess, E.W., R.R. Forster, C.F. Larsen, and M. Braun, 2012: Surge dynamics of Bering Glacier, Alaska, in 2008–2011. *The Cryosphere*, **6**, 1251–1262, DOI:10.5194/tc-6-1251-2012.

Butler, D.R., and L.M. DeChano, 2001: Environmental change in Glacier National Park, Montana: An assessment through repeat photography from fire lookouts. *Physical Geography*, **22**, 291–304.

Cox, L.H., and R.S. March, 2004: Comparison of geodetic and glaciological mass-balance techniques, Gulkana Glacier, Alaska, U.S.A. *Journal of Glaciology*, **50**, 363–370, DOI:10.3189/172756504781829855.

Dahlman, L., 2009: Climate variability: Arctic Oscillation. NOAA, Accessed 7 May 2021, https://www.climate.gov/news-features/understanding-climate/climate-variability-arctic-oscillation.

Dunse, T., T. Schellenberger, J.O. Hagen, A. Kääb, T.V. Schuler, and C.H. Reijmer, 2015: Glacier-surge mechanisms promoted by a hydro-thermodynamic feedback to summer melt. *The Cryosphere*, **9**, 197–215, DOI:10.5194/tc-9-197-2015.

ESRI Inc., 2019: ArcGIS Pro, Version 2.4.0. ESRI Inc., https://www.esri.com/en-us/arcgis/products/arcgis-pro/overview.

Field, W.O., Jr., 1947: Glacier recession in Muir Inlet, Glacier Bay, Alaska. *Geographical Review*, **37**, 369–399, DOI:10.2307/211127.

Fleming, S.W., and P.H. Whitfield, 2010: Spatiotemporal mapping of ENSO and PDO surface meteorological signals in British Columbia, Yukon, and southeast Alaska. *Atmosphere-Ocean*, **48**, 122–131, DOI:10.3137/AO1107.2010.

Fountain, A.G., and J.S. Walder, 1998: Water flow through temperate glaciers. *Reviews of Geophysics*, **36**, 299–328, DOI:10.1029/97RG03579.

GlacierChange.org, 2011: Mendenhall Glacier: Repeat photography. Accessed 24 November 2019, http://glacierchange.org/scrapbook/mendenhall-glacier/mendenhall-gallery/.

Harrison, W.D., and A.S. Post, 2003: How much do we really know about glacier surging?. *Annals of Glaciology*, **36**, 1–6, DOI:10.3189/172756403781816185.

Hayes, M.O., C.H. Ruby, M.F. Stephen, and S.J. Wilson, 1976: Geomorphology of the southern coast of Alaska. *Coastal Engineering 1976*, 1992–2008, DOI:10.1061/978087262034.

Hendrick, L.E., and C.A. Copenheaver, 2009: Using repeat landscape photography to assess vegetation changes in rural communities of the southern Appalachian Mountains in Virginia, USA. *Mountain Research and Development*, **29**, 21–29, DOI:10.1659/mrd.1028.

Hodge, S.M., D.C. Trabant, R.M. Krimmel, T.A. Heinrichs, R.S. March, and E.G. Josberger, 1998: Climate variations and changes in mass of three glaciers in western North America. *Journal of Climate*, **11**, 2161–2179, DOI:10.1175/1520-0442(1998)011<2161:CVAC1M>2.0CO;2.

Humphrey, N.F., and C.F. Raymond, 1994: Hydrology, erosion and sediment production in a surging glacier: Variegated Glacier, Alaska, 1982–83. *Journal of Glaciology*, **40**, 539–552, DOI:10.3189/S0022143000012429.

Jacquemart, M., M. Loso, M. Leopold, E. Welty, E. Berthier, J.S.S. Hansen, J. Sykes, and K. Tiampo, 2020: What drives large-scale glacier detachments? Insights from Flat Creek glacier, St. Elias Mountains, Alaska. *GEOLOGY*, **48**, 703–707, DOI:10.1130/G47211.1.

Lambrou, E., and G. Pantazis, 2006: A new geodetic methodology for the accurate documentation and monitoring of inaccessible surfaces. *Proc. 12th FIG Symposium on Deformation Measurements*, Baden, Austria, International Federation of Surveyors, https://www.fig.net/resources/proceedings/2006/baden_2006_comm6/PDF/O3D/Lambrou.pdf.

Larsen, C.F., R.J. Motyka, J.T. Freymueller, K.A. Echelmeyer, and E.R. Ivins, 2004: Rapid uplift of southern Alaska caused by recent ice loss. *Geophysical Journal International*, **158**, 1118–1133, DOI:10.1111/j.1365-246X.2004.02356.x.

Larsen, C.F., E. Burgess, A.A. Arendt, S. O'Neel, A.J. Johnson, and C. Kienholz, 2015: Surface melt dominates Alaska glacier mass balance. *Geophysical Research Letters*, **42**, 5902–5908, DOI:10.1002/2015GL064349.

Lingle, C.S., A. Post, U.C. Herzfeld, B.F. Molnia, R.M. Krimmel, and J.J. Roush, 1993: Bering Glacier surge and iceberg-calving mechanism at Vitus Lake, Alaska, U.S.A.. *Journal of Glaciology*, **39**, 722–727, DOI:10.3189/S0022143000016683.

Lluch-Cota, D.B., W.S. Wooster, and S.R. Hare, 2001: Sea surface temperature variability in coastal areas of the Northeastern Pacific related to the El Niño-Southern Oscillation and the Pacific Decadal Oscillation. *Geophysical Research Letters*, **28**, 2029–2032, DOI:10.1029/2000GL012429.

Massonnet, D., and K.L. Feigl, 1998: Radar interferometry and its application to changes in the earth's surface. *Reviews of Geophysics*, **36**, 441–500, DOI:10.1029/97RG03139.

Melkonian, A.K., M.J. Willis, and M.E. Pritchard, 2014: Satellite-derived volume loss rates and glacier speeds for the Juneau Icefield, Alaska. *Journal of Glaciology*, **60**, 743–760, DOI:10.3189/2014JoG13J181.

Menounos, B., and Coauthors, 2019: Heterogeneous changes in western North American glaciers linked to decadal variability in zonal wind strength. *Geophysical Research Letters*, **46**, 200–209, DOI:10.1029/2018GL080942.

Motyka, R.J., S. O'Neel, C.L. Connor, and K.A. Echelmeyer, 2002: *Global and Planetary Change*, **35**, 93–112, DOI:10.1016/S0921-8181(02)00138-8.

Murray, T., and Coauthors, 2015: Dynamics of glacier calving at the ungrounded margin of Helheim Glacier, southeast Greenland. *Journal of Geophysical Research: Earth Surface*, **120**, 964–982, DOI:10.1002/2015JF003531.

National Park Service, 2017: Repeat photography: Capturing change. Accessed 28 October 2019, https://www.nps.gov/glba/learn/nature/time-lapse-sliders.htm.

Neal, E.G., M.T. Walker, and C. Coffeen, 2002: Linking the pacific decadal oscillation to seasonal stream discharge patterns in Southeast Alaska. *Journal of Hydrology*, **263**, 188–197, DOI:10.1016/S0022-1694(02)00058-6.

Nicholls, R.J., and A. Cazenave, 2010: Sea-level rise and its impact on coastal zones. *Science*, **328**, 1517–1520, DOI:10.1126.science.185782.

NOAA/NCDC, 2021a: Arctic Oscillation (AO). NOAA/National Climatic Data Center. Subset used: September 1970–August 2018, accessed 25 March 2021, https://www.ncdc.noaa.gov/teleconnections/ao/.

NOAA/NCDC, 2021b: Pacific Decadal Oscillation (PDO). NOAA/National Climatic Data Center. Subset used: September 1970–August 2018, accessed 25 March 2021, https://www.ncdc.noaa.gov/teleconnections/pdo/.

NOAA/NCDC, 2021c: Southern Oscillation Index (SOI). NOAA/National Climatic Data Center. Subset used: September 1970–August 2018, accessed 25 March 2021, https://www.ncdc.noaa.gov/teleconnections/enso/indicators/soi/.

NOAA/NCEI, 2021a: Auke Bay, AK US Daily Summaries. NOAA/National Centers for Environmental Information. Subset used: June 1970–August 2018, accessed 25 March 2021, https://www.ncdc.noaa.gov/cdo-web/datasets/GHCND/stations/GHCND:USC00500464/detail.

NOAA/NCEI, 2021b: Extended Reconstructed Sea Surface Temperature (ERSST), Version 4. NOAA/National Centers for Environmental Information. Subset used: September 1970–August 2018, accessed 12 March 2021, https://www.ncdc.noaa.gov/data-access/marineocean-data/extended-reconstructed-sea-surface-temperature-ersst-v4.

Nolan, M., A. Arendt, B. Rabus, and L. Hinzman, 2005: Volume change of McCall Glacier, Arctic Alaska, USA, 1965–2003. *Annals of Glaciology*, **42**, 409–416, DOI:10.3189/17275640578182943.

NSIDC, 2020a: How are glaciers formed?. Accessed 7 May, 2021, https://nsidc.org/cryosphere/glaciers/questions/formed.html.

NSIDC, 2020b: What is the Arctic Oscillation?. Accessed 7 May, 2021, https://nsidc.org/cryosphere/icelights/2012/02/arctic-oscillation-winter-storms-and-sea-ice.

Paul, F., and Coauthors, 2015: The glaciers climate change initative: Methods for creating glacier area, elevation change and velocity products. *Remote Sensing of Environment*, **162**, 408–426, DOI:10.1016/j.rse.2013.07.043.

Quincey, D.J., and Coauthors, 2014: Digital terrain modeling and glacier topographic characterization. In *Global Land Ice Measurements from Space*, Springer-Verlag, 113–144, DOI:10.1007/978-3-540-79818-7_5.

Rapp, A., 1996: Photo documentation of landscape change in northern Swedish mountains. *Ecological Bulletins*, **45**, 170–179.

Rasmussen, L.A., and H. Conway, 2005: Influence of upper-air conditions on glaciers in Scandinavia. *Annals of Glaciology*, **42**, 402–408, DOI:10.3189/17275604578182727.

Rignot, E., J. Mouginot, and B. Scheuchl, 2011: Ice flow of the Antarctic ice sheet. *Science*, **333**, 1427–1430, DOI:10.1126/science.1208336.

Schoof, C., 2010: Ice-sheet acceleration driven by melt supply variability. *Nature*, **468**, 803–806, DOI:10.1038/nature09618.

Sevestre, H., and D.I. Benn, 2015: Climatic and geometric controls on the global distribution of surge-type glaciers: Implications for a unifying model of surging. *Journal of Glaciology*, **61**, 646–662, DOI:10.3189/2015JoG14J136.

Sharp, R.P., 1951: Accumulation and ablation on the Seward-Malaspina glacier system, Canada-Alaska. *Bulletin of the Geological Society of America*, **62**, 725–744, DOI:10.1130/0016-7606(1951)62[725:AAAOTS]2.0.CO;2.

Steiner, D., A. Pauling, S.U. Nussbaumer, A. Nesje, J. Luterbacher, H. Wanner, and H.J. Zumbühl, 2008: Sensitivity of European glaciers to precipitation and temperature – two case studies. *Climate Change*, **90**, 413–441, DOI:10.1007/s10584-008-9393-1.

Trabant, D.C., and L.R. Mayo, 1985: Estimation and effects of internal accumulation on five glaciers in Alaska. *Annals of Glaciology*, **6**, 113–117, DOI:10.3189/1985AoG6-1-113-117.

USGS/Earth Resources Observation and Science (EROS) Center, 2021a: Landsat 1-5 MSS C2 L1. USGS Earth Explorer, https://earthexplorer.usgs.gov/.

USGS/Earth Resources Observation and Science (EROS) Center, 2021b: Landsat 4-5 TM C2 L2. USGS Earth Explorer, https://earthexplorer.usgs.gov/.

USGS/Earth Resources Observation and Science (EROS) Center, 2021c: Landsat 7 ETM+ C2 L2. USGS Earth Explorer, https://earthexplorer.usgs.gov/.

USGS/Earth Resources Observation and Science (EROS) Center, 2021d: Landsat 8 OLI/TIRS C2 L2. USGS Earth Explorer, https://earthexplorer.usgs.gov/.

VanLooy, J.A., and G.S. Vandeberg, 2019: Late summer glacial meltwater contributions to Bull Lake Creek stream flow and water quality, Wind River Range, Wyoming, USA. *Physical Geography*, **40**, 461–480, DOI:10.1080/02723646.2019.1565215.

Xu, J., R.E. Grumbine, A. Shrestha, M. Eriksson, X. Yang, Y. Wang, and A. Wilkes, 2009: The melting Himalayas: Cascading effects of climate change on water, biodiversity, and livelihoods. *Conservation biology: the journal of the Society for Conservation Biology*, **23**, 520–530, DOI:10.1111/j.1523-1739.2009.01237.x.

Yao, X., J. Iqbal, L.-J. Li, and Z.-K. Zhou, 2019: Characteristics of mountain glacier surge hazard: Learning from a surge event in NE Pamir, China. *Journal of Mountain Science*, **16**, 1515–1533, DOI:10.1007/s11629-018-5282-x.

Zheng, W, M.E. Pritchard, M.J. Willis, and L.A. Stearns, 2019: The possible transition from glacial surge to ice stream on Vavilov Ice Cap. *Geophysical Research Letters*, **46**, 13892–13902, DOI: 10.1029/2019GL094948.